Article

Not peer-reviewed version

Mineralogy and, Major and Trace Elements Chemistry of Recent Sediments in Rivers Along the West Coast of India: Implications for Provenance and Chemical Weathering

Sk Sai Babu , Venigalla Purnachandra Rao * , Mekala Ram Mohan

Posted Date: 11 October 2024

doi: 10.20944/preprints202410.0793.v1

Keywords: fluvial sediments; trace elements; Western Ghats; Deccan Trap terrain; Archean-Proterozoic terrain; chemical weathering; provenance

Article

Mineralogy and, Major and Trace Elements Chemistry of Recent Sediments in Rivers Along the West Coast of India: Implications for Provenance and Chemical Weathering

Sk. Sai Babu [1], V. Purnachandra Rao [1,*] and M. Ram Mohan [2]

[1] Vignan's Foundation for Science, Technology and Research (VFSTR), Deemed to be Vignan's University. Vadlamudi, Guntur, 522 213, Andhra Pradesh, India.
[2] CSIR-National Geophysical Research Institute, Uppal Road, Hyderabad, 500 007, Telangana, India
* Correspondence: vprao55@gmail.com

Abstract: The sediments deposited at the lower reaches of 90 medium and minor rivers from 5 states along western India were analysed for mineralogy and, major and trace elements chemistry. Kaolinite followed by minor illite and gibbsite and traces of goethite and, smectite followed by minor kaolinite, illite and chlorite are characteristic of the clays from Archean-Proterozoic (A-P) terrain and Deccan Trap (DT) terrain, respectively. The sediments were depleted with Si, Ca, Mg, Na and K relative to that of Post Archean average Australian Shale. The SiO_2/Al_2O_3 ratio suggests the sediments from A-P terrain resemble lateritic soils, while those from DT terrain are non-lateritic, chemically weathered soils. The weathering indices indicate intensely weathered and compositionally mature sediments from Kerala, Karnataka and Maharashtra and, intermediate to intensely weathered sediments from Goa and Gujarat. The sediments exhibit relatively high Th, U, La, Zr and Hf from A-P terrain and, high Sc, Cr, Co, Ni, V and Ga from DT terrain. The total trace element content (∑TE) was lower for the clay than silt fractions of sediments. The peak high ∑TE occur in the silt fraction of sediments from Kerala and Maharashtra. The Th/U and Rb/Sr ratios are controlled by the intensity of weathering and lithology of source rocks. The standard plots using trace elements reveal intermediate provenance between felsic and mafic source. Clay fractions from both terrains are more mafic implying mafic-component dominated sediments are transported to the adjacent Seas and Oceans. Therefore, it would be challenging to identify the clays transported from granitic terrain in the Oceans, using trace element chemistry.

Keywords: fluvial sediments; trace elements; Western Ghats; Deccan Trap terrain; Archean-Proterozoic terrain; chemical weathering; provenance

1. Introduction

Rivers are the most significant dynamic systems, which erode the Earth's surface and transport weathered continental material to the oceans. The composition of river sediment can be influenced by factors such as the type of source rocks, climate, low and high relief, degree of chemical weathering, transport, and post-depositional diagenetic effects (Nesbitt and Young, 1982; Nesbitt et al., 1996; Taylor and McLennan, 1985; McLennan, 1989; McLennan et al., 1993; Fedo et al., 1995; Selvaraj and Chen, 2006; Borges et al., 2008; Liu et al., 2012; Lupker et al., 2013; Garzanti and Resentini, 2016; Hossain et al., 2018). The river sediments thus provide cumulative information on the composition of the continental crust, impact of weathering, tectonic setting of the source terrain and sedimentary processes associated with transportation and deposition (Roser and Korsch, 1986, 1988; Amajor, 1987; Cox et al., 1995; Hayashi et al., 1997; Roy and Roser, 2013; Armstrong-Altrin et al., 2021; Hossain, 2020; Boruah and Laskar, 2022). It is, however, possible to point out the influence of these parameters from the mineral and chemical characteristics of sediments. For example, high precipitation and intense chemical weathering are typical in humid, tropical climatic conditions. Chemical weathering not only affects global climate by consuming atmospheric carbon-dioxide by silicate weathering (Berner and Berner, 1997; Kump et al., 2000), but also causes chemical degradation of rocks resulting in high dissolved load of mobile elements and enrichment of immobile elements in the sediments and, high sediment yield into the rivers. The erosional products of chemical weathering are finer than those derived from physical or mechanical weathering. Topography influences the sediment characteristics. For instance, the steep slopes promote more of physical weathering and produce coarser sediment. Sediment texture, mineralogy and chemistry are modified by hydraulic sorting processes. Post-depositional processes such as diagenesis modify the sediment composition depending on oxic, sub-oxic and anoxic conditions in the sediments. However, recent sediments exhibit little or no diagenetic effect on sediment composition (Chamley, 1989).

Numerous studies have been carried out on mineralogy and geochemistry of the sediments from large as well as small rivers to better understand the provenance and impact of chemical weathering on source rocks (Sarma and Rajamani 2001; Selvaraj and Chen 2006; Sen Sarma et al., 2008; Bhuiyan et al., 2011; Maharana et al., 2018; He et al., 2020; Hossain, 2020, Rahman et al., 2020; Chougong et al., 2021; Sai Babu et al., 2020, 2021, 2023, 2024; Saha et al., 2023; Guo et al., 2023; Gurumurthy, 2024). The studies indicate that the sediments deposited by small rivers are of considerable importance as they are good indicators of weathering environment typical of their basins and help to constrain the nature of source rocks (Mahle, 2023). The sediment mineralogy and major element chemistry (mobile and easily leachable elements) have been used to deduce the weathering history (Cullers, 1994; Price and Velbel, 2003), while immobile trace elements, such as La, Zr, Sc, Cr, V, Th, Hf, and Yb during sediment transport and diagenesis provide valuable information on provenance (Cullers, 1994; Wronkiewicz and Condie,1989; Bhatia, 1983; Hayashi et al., 1997). In this study, we have investigated mineralogical and, major and trace element characteristics of sediments deposited at the lower reaches of the medium and minor rivers (Rao, 1975) along the west coast of India. These rivers drain the Western Ghats (WG) that comprise of two distinct geological formations all along its length and experience humid, tropical climate. The western slope of the WG is much steeper in the northern and southern part than in the central part. The basement rocks of the WG are covered by laterites, whose thickness decreases considerably from south to north. Several investigators reported the mineralogy and geochemistry of the suspended and/or bed sediments of the rivers and/or estuaries (Naidu et al., 1985; Subramanian et al., 1985; Ramesh et al., 1989; Singh and Rajamani, 2001; Das and Krishnaswamy, 2007; Sen Sarma et al., 2008; Sharma, 2013; Sai Babu et al., 2021, 2024; Shynu et al., 2011, 2013, 2017, Prajith et al., 2015, Kessarkar et al., 2003, 2015; Babechuk et al., 2014, 2015, 2022; Gurumurthy, 2024) or mineral composition of the sediments in the adjacent continental shelf (Rao and Rao, 1995; Kessarkar et al., 2003). The purpose of the study is to report clay minerals, major and trace element characteristics of sediments in rivers along the west coast of India and investigate the factors controlling sediment composition.

2. Geological Setting

Geomorphology: The present study is on the mineralogy, major and trace elements chemistry of sediments in 90 medium and minor rivers along the west coast of India (Figure 1). These rivers receive sediment load and waters from the Western Ghats (WG; mountain range), a linear geomorphic feature that runs parallel to the west coast of India (Figure 1; Krishnan, 1968). The Western Ghats starts near the border of Gujarat and Maharashtra, south of the Tapti River and runs ~1600 km through the states of Maharashtra, Goa, Karnataka, Kerala and Tamil Nadu and ends at Kanyakumari. The northern Western Ghats (Gujarat through Maharashtra up to Goa) with steep gradient are remarkably straight and lie at the edge of the Arabian Sea, also known as the Great Escarpment of India (Widdowson and Cox, 1996, Kale, 2009). Here, the Ghats exhibit rugged topography, steep cliffs, deep valleys and dense forests. The Ghats are further inland, 50 to 80 km away from the seashore between Bhatkal and Cochin in the central and southern part and, again located on the coast in the south Kerala and around Tiruvunanthapuram. The height of the Western

Ghats is up to 2600 m, with an average elevation of ~1200 m and, their width varies between 50 and 80 km.

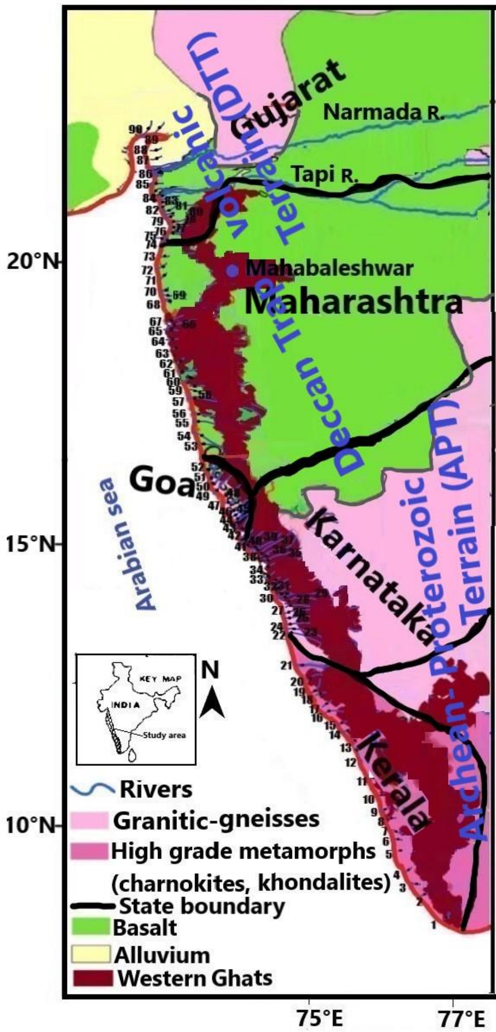

#	River Name (Length (km))	#	River Name (Length (km))
1	Neyyar (56)	46	Mandovi (81)
2	Vamanpuram (88)	47	Mapusa (20)
3	Ithikkara (56)	48	Nerul (17)
4	Kallada (120)	49	Baga (15)
5	Achankovil (128)	50	Anjuna (19)
6	Pamba (176)	51	Chapora (21)
7	Manimalayar (90)	52	Terikhol (28)
8	Meenachil (78)	53	Mochemaad (27)
9	Muvattupuzha (121)	54	Mandavi (12)
10	Periyar (244)	55	Karli (14)
11	Chalakudi (145)	56	Gad (66)
12	Karuvannur (45)	57	Naringre (27)
13	Bharathapuzha (209)	58	Vaghotan (40)
14	Kadalundy (130)	59	Arjuna (37)
15	Chaliyar (169)	60	Muchkundi (59)
16	Kuttyadi (74)	61	Gautami (29)
17	Mahe (54)	62	Kajali (37)
18	Valapatanam (110)	63	Jaigad (42)
19	Kuppam (88)	64	Vashisti (35)
20	Thejaswini (64)	65	Bharja (27)
21	Chandragiri (105)	66	Savitri (110)
22	Netravati (103)	67	Kundalika (74)
23	Gurupura (30)	68	Amba (63)
24	Nandini (103)	69	Bhogavati (52)
25	Shambavi (60)	70	Patalganga (16)
26	Pangala (37)	71	Tansa (16)
27	Udyavara (27)	72	Vaitarna (154)
28	Suvarna (88)	73	Surya (21)
29	Sita (50)	74	Bananga (17)
30	Haladi (70)	75	Darotha (27)
31	Kolluru (38)	76	Daman Ganga (131)
32	Yadamavu (32)	77	Par (51)
33	Uppunda (27)	78	Wanki (17)
34	Venkatapur (50)	79	Auranga (97)
35	Pallinadu (42)	80	Kharera (40)
36	Alvekodi (27)	81	Ambika (136)
37	Sharavati (128)	82	Purna (180)
38	Badagani (21)	83	Mindhola (105)
39	Agnashini (117)	84	Tapi (724)
40	Gangavali (152)	85	Kim (107)
41	Kali (184)	86	Narmada (1312)
42	Galgibaga (15)	87	Viswamitri (142)
43	Talpona (31)	88	Mahi (583)
44	Sal (35)	89	Sabarmati (371)
45	Zuari (34)	90	Bhogawo (120)

Fig. 1

Figure 1. Map of the West Coast of India. Rivers investigated in this study are numbered. Dots mark the sample location in each river. Location of the Western Ghats along the coast and basic geology of western India are also shown in the map. States and state boundaries are marked. Major rivers (Narmada and Tapi) are also shown.

Geology: The Western Ghats comprise of two broad and predominant geological formations, the continental flood basalts (Deccan Traps) in the north and Archean-Proterozoic formations in the south (Figure 1; Krishnan, 1968). The flood basalts cover vast areas (>500,000 km^2) for the Deccan and represent the extrusion of phenomenal volumes of lava. The thickness of the Deccan Traps varies considerably (200 m to 2 km) with its maximum in the plateau region. The thickness and number of discrete lava flows is greatest in the western parts and decreasing gradually towards east and south. The Deccan Trap basalts can be divided into 4 stratigraphic subdivisions. The lower basalts (the Bushe and Poladpur formations) are largest and show evidence of contamination with upper crustal material. The upper basalts (the Ambenali and Mahabaleshwar formations) show low contamination and/or mobilization of material from the mantle lithosphere (Lightfoot et al., 1990). The lateral transition from the Deccan basalts to Archean-Proterozoic formations (APF) occurs close to the border of Maharashtra and Goa (Figure 1). The APF can further be divided into granites and gneisses in the north and high-grade charnockites and khondalites in the south (Radhakrishna, 1983; Figure 1). The basement rocks of Goa and Karnataka belong to the Dharwar Super Group (Gokul et al., 1985)

Preprints.org (www.preprints.org) | NOT PEER-REVIEWED | Posted: 11 October 2024 doi:10.20944/preprints202410.0793.v1

with green schists and gneisses. The iron and manganese ore deposits occur in Goa and are being mined by open cast method (Gokul et al., 1985, Mascarenhas and Kalavampara, 2009). The Mandovi and Zuari Rivers drain through these ore deposits and carry ore particulates in their suspended and bed loads (Shynu et al., 2011, 2013). Supergene Mn ore deposits formed on Late Archean rocks also occur in the northern Karnataka (Jean et al., 2020). Cryptomalene (K-rich, Mn-oxide) is a predominant mineral in the deposits. Limestones, dolomites, ultramafic rocks, orthoquartzites, argillite, banded magnetite/ hematite quartzites are minor rock types of Karnataka. Laterites cover extensively the basement rocks of the Western Ghats at different topographic levels between Kerala and Maharashtra. The thickness of the laterites is several tens of meters (up to 30 m) in Kerala, Karnataka and Goa and decreases to < 10 m in the Deccan Trap (Maharashtra) region (Kaotekwar et al., 2014). Bauxite deposits are reported at several locations in the Kerala.

Climate: Humid, tropical climate prevails all along the Western Ghats. Semi-arid climate is prevalent in the north of Narmada and Tapti Rivers and Gujarat (Krishnan 1968; Sreenath et al. 2022). The mountain ranges intercept the rain-bearing westerly winds during the southwest monsoon (June–September). Consequently, the western slopes of the Western Ghats receive far more rainfall (av. 250 cm/yr) than their eastern slopes (100 cm/yr). Precipitation is much heavier with an average rainfall of 300–400 cm/yr in the states of Maharashtra, Goa and northern Karnataka than the southern Karnataka and Kerala. Numerous medium and minor rivers draining the western slope of the Western Ghats (Figure 1) are fast-moving, owing to short distance travelled and steeper gradient and bring suspended and bed load of sediment into the Arabian Sea.

3. Materials and Methods

Numerous rivers drain the western slopes of the Western Ghats and bring sediments to the coastal Arabian Sea. For this study, sediments were collected at the lower reaches of 90 rivers from 5 states, between Neyyar River of Kerala and Bhogawa River of Gujarat (Figure 1), using Van Veen Grab. The sediments recovered were dried. The sediments from the rivers of Kerala, Karnataka and Goa are considered and derived from Archean- Proterozoic (A-P) terrain and those from Maharashtra and Gujarat are from Deccan Trap (DT) terrain. The sand, silt and clay fractions of sediments were separated in the laboratory, following Folk (1968). The < 62 μm fraction of the sediment was separated from the total sediment by wet sieving, using 230 (ASTM) mesh sieve. This fraction was collected in a measuring glass cylinder, made up to 1000 ml volume with distilled water and stirred vigorously for homogeneity. The <4 μm fraction (clay) was separated based on Stoke's settling velocity and collected in a beaker, dried in an oven at 60° C and then powdered. This procedure was repeated several times and ensured that the clay fraction was removed completely from the <62 μm fraction of sediment in the cylinder. Then the remaining fraction was dried and powdered, as it represents silt fraction (>4 to 62 μm). The powdered sediment size fractions were used for geochemical analyses.

The major elements were determined on clay and silt fractions of sample powders by using X-ray Fluorescence spectrometer, 'WD XRF' Model Axios mAX4, P-Analytical, at CSIR-National Geophysical Research Institute (CSIR-NGRI), Hyderabad. A detailed procedure was given in Sai Babu et al. (2021). For trace and rare earth element analysis, the detailed procedure mentioned in Sai Babu et al. (2024) was used and also repeated below: A 50 mg of sample powders were taken in Savillex vessels to which 10 ml of acid mixture containing hydrofluoric acid (HF) and nitric acid (HNO_3) in 7:3 ratio. These vials were tightly closed and were heated at 150° C for 48 hours. Following this step, these vials were opened and heated at 100° C to near dryness. The sample residue was further mixed with 10 ml of acid mixture containing nitric acid (HNO_3) and Millipore water in 1:1 ratio and was heated at 80° C for 1 hour. To obtain the necessary TDS level, and to minimize the matrix effects, the obtained sample solution was diluted 50,000 times. Trace elements were determined by High-Resolution Inductively Coupled Plasma Mass Spectrometer (HR-ICP-MS, Attom), Nu Instruments at CSIR-NGRI, Hyderabad. The instrument drift was monitored and corrected using ^{103}Rh as the internal standard. The within run RSD for all the analysed elements were under 3%. Certified reference material JSD-3 μg/g was repeatedly analysed as an unknown to monitor the accuracy and reproducibility of the obtained trace element data.

Preprints.org (www.preprints.org) | NOT PEER-REVIEWED | Posted: 11 October 2024 doi:10.20944/preprints202410.0793.v1

Table 1 shows the major element data of the clay and silt fractions of sediments and, data on weathering indices such as chemical index of alteration (CIA; Nesbitt and Young, 1996), plagioclase index of alteration (Fedo et al., 1995), Index of chemical variability (Cox et al., 1995) and mafic index of alteration (MIA: Babechuk et al., 2014) and index of laterization (IOL; Babechuk et al. 2022). Trace elements data for the clay and silt fractions of sediments are given in Table 2 and Table 3, respectively. Table 4 shows correlation matrix for the clay fraction of sediments, separately for Archean-Proterozoic terrain (APT) and Deccan Trap terrain (DTT).

Preprints.org (www.preprints.org) | NOT PEER-REVIEWED | Posted: 11 October 2024 doi:10.20944/preprints202410.0793.v1

Table 1. Major elements content (%) of the clay (<4 μm) and silt (>4 to 63 μm) fraction of sediments in the rivers of West coast of India.

State (No. of Rivers)		SiO_2	Al_2O_3	Fe_2O_3	MnO	MgO	CaO	Na_2O	K_2O	TiO_2	P_2O_5	SiO_2/Al_2O_3	Fe_2O_3/Al_2O_3	Al_2O_3/TiO_2	CIA	PIA	ICV	MIA (O)	MIA (R)	IOL
Kerala (21)	Range	29.01-40.66	11.37-32.01	7.39-15.27	0.05-0.22	0.65-3.70	0.25-2.96	0.16-25.28	0.68-2.88	0.71-1.44	0.15-0.83	1.05-2.91	0.35-0.82	11.42-37.04	26.95-96.35	20.82-93.92	0.44-3.76	38.75-95.87	21.72-72.67	35.12-57.04
	Avg.	34.24	23.59	11.84	0.12	1.69	0.68	2.82	1.18	1.11	0.45	1.45	0.50	21.22	86.10	79.69	0.97	85.84	58.07	50.57
	STD (±)	2.94	4.48	2.12	0.05	0.81	0.59	7.22	0.57	0.22	0.16	0.48	0.11	6.72	19.04	20.61	0.78	15.74	12.61	5.61
Karnataka (20)	Range	37.88-52.33	18.09-21.88	6.32-17.33	0.02-0.34	0.29-2.76	0.11-0.85	0.06-1.04	0.51-1.64	0.89-1.80	0.10-0.40	1.91-2.54	0.31-0.95	11.73-20.38	84.49-96.60	76.90-94.35	0.51-1.24	83.14-97.07	48.16-71.78	33.94-48.13
	Avg.	43.12	19.43	12.39	0.08	1.18	0.42	0.44	1.09	1.23	0.26	2.22	0.64	16.35	90.87	85.76	0.87	91.08	58.00	42.52
	STD (±)	3.86	1.03	2.86	0.07	0.61	0.20	0.35	0.33	0.26	0.08	0.14	0.17	2.79	2.86	4.22	0.19	3.27	6.13	3.66

Preprints.org (www.preprints.org) | NOT PEER-REVIEWED | Posted: 11 October 2024 doi:10.20944/preprints202410.0793.v1

Goa (11)	Range	36.14-43.11	15.61-21.66	9.67-17.71	0.04-0.58	1.21-3.87	0.29-1.33	0.56-8.40	1.28-1.63	1.01-1.97	0.17-0.49	1.82-2.57	0.50-1.13	9.23-15.94	61.49-88.35	55.96-81.79	0.83-1.61	70.30-90.49	41.30-59.13	40.61-47.97
	Avg.,	40.06	18.05	13.20	0.16	2.45	0.72	2.33	1.49	1.36	0.32	2.24	0.74	13.71	80.97	74.25	1.21	82.19	49.21	43.81
	STD (±)	2.27	1.95	2.01	0.17	0.73	0.33	2.57	0.12	0.32	0.09	0.22	0.16	2.03	8.52	7.99	0.24	6.06	5.43	2.68
Archean- Proterozoic Terrain (APT)	Range	29.01-52.33	11.37-32.01	6.32-17.71	0.04-0.58	0.65-3.87	0.11-2.96	0.06-25.28	0.51-2.88	0.71-1.97	0.10-0.83	1.05-2.91	0.31-1.13	9.23-37.04	26.95-96.60	20.82-94.35	0.44-3.76	38.75-97.07	21.72-72.67	33.94-57.04
	Avg.,	38.89	20.82	12.34	0.11	1.65	0.59	1.80	1.21	1.21	0.35	1.95	0.61	18.10	85.98	79.90	1.01	86.37	55.09	45.63
	STD (±)	5.11	3.82	2.42	0.10	0.85	0.44	4.79	0.44	0.27	0.15	0.47	0.17	5.77	10.14	10.94	0.40	8.35	7.10	5.97
Maharashtra (21)	Range	28.32-51.21	13.71-21.65	3.13-14.67	0.07-0.44	0.79-5.72	0.26-2.10	0.12-13.22	0.55-1.34	0.63-2.98	0.06-0.54	1.87-3.32	0.14-0.88	7.27-29.27	48.67-94.06	45.86-91.36	0.42-2.13	61.96-93.91	34.01-79.08	31.52-47.59

	Avg.,	42.28	16.90	10.75	0.18	2.23	1.07	1.09	0.91	1.51	0.25	2.54	0.65	11.98	85.19	80.59	1.08	84.23	53.51	39.66
	STD (±)	4.74	2.28	2.51	0.10	1.20	0.53	2.79	0.29	0.44	0.10	0.42	0.18	4.33	9.25	9.28	0.34	7.09	9.06	4.13
Gujarat (17)	Range	42.88-50.36	13.04-16.24	6.13-10.57	0.10-0.24	2.51-4.29	1.65-6.38	0.18-1.31	0.66-1.83	0.99-2.20	0.11-0.36	2.71-3.77	0.38-0.76	7.38-16.10	61.78-84.19	53.70-80.76	0.87-1.65	63.94-82.35	39.99-58.96	30.16-37.18
	Avg.,	47.35	14.43	8.91	0.15	3.39	3.05	0.54	1.29	1.44	0.17	3.29	0.62	10.39	75.02	68.39	1.31	74.02	47.15	33.05
	STD (±)	2.49	0.85	1.09	0.030	0.48	1.05	0.36	0.37	0.29	0.07	0.29	0.09	2.05	5.42	6.70	0.17	4.32	4.10	2.10
Deccan Trap Terrain (DTT)	Range	28.32-51.21	13.04-21.65	3.13-14.67	0.07-0.44	0.79-5.72	0.26-6.38	0.12-13.22	0.55-1.83	0.63-2.98	0.06-0.54	1.87-3.77	0.14-0.88	7.27-29.27	48.67-94.06	45.86-91.36	0.42-2.13	61.96-93.91	34.01-79.08	30.16-47.59
	Avg.,	44.55	15.79	9.93	0.17	2.75	1.96	0.84	1.08	1.48	0.21	2.88	0.64	11.27	80.10	74.49	1.19	79.12	50.33	36.35
	STD (±)	4.63	2.16	2.19	0.08	1.11	1.28	2.08	0.38	0.38	0.10	0.53	0.14	3.55	7.33	7.99	0.25	5.70	5.12	3.11

West Coast of India River Average Clay (WCIRAC)	Range	28.32-52.33	11.37-32.01	3.13-17.71	0.65-5.72	0.11-6.38	0.06-25.28	0.51-2.88	0.01-2.98	0.04-0.58	0.06-0.83	1.05-3.77	0.14-1.13	7.26-37.05	26.95-96.60	20.82-94.35	0.42-3.76	38.75-97.07	21.72-79.08	30.16-48.13
	Avg.	41.41	18.69	11.32	2.20	1.27	1.32	1.15	1.32	0.13	0.29	2.34	0.63	15.21	83.63	78.98	1.06	83.94	54.12	41.92
	STD (±)	3.26	4.06	2.60	0.98	0.86	3.43	0.42	0.34	0.09	0.14	0.31	0.14	5.98	9.01	12.87	0.47	10.40	9.51	2.63

Silt

State (No. of Rivers)		SiO_2	Al_2O_3	Fe_2O_3	MnO	MgO	CaO	Na_2O	K_2O	TiO_2	P_2O_5	SiO_2/Al_2O_3	Fe_2O_3/Al_2O_3	Al_2O_3/TiO_2	CIA	PIA	ICV	MIA (O)	MIA (R)	IOL
Kerala (21)	Range	34.08-48.17	15.44-26.06	9.55-16.03	0.06-0.22	0.60-3.53	0.30-2.59	0.17-1.89	0.72-2.66	0.74-1.57	0.15-0.80	1.38-2.21	0.37-0.71	11.29-34.19	76.13-94.19	67.23-91.28	0.57-1.14	75.61-93.55	50.39-67.10	34.69-54.21
	Avg.	38.75	22.71	12.09	0.13	1.71	0.94	0.49	1.54	1.24	0.41	1.71	0.53	18.31	88.36	82.33	0.81	88.09	59.34	47.37
	STD (±)	3.96	2.25	1.94	0.04	0.75	0.52	0.36	0.55	0.22	0.14	0.35	0.10	4.64	4.25	5.95	0.16	4.20	4.94	4.02

Preprints.org (www.preprints.org) | NOT PEER-REVIEWED | Posted: 11 October 2024 doi:10.20944/preprints202410.0793.v1

Karnataka (20)	Range	39.34-65.74	15.21-21.44	6.69-13.39	0.02-0.13	0.34-2.21	0.07-1.18	0.05-0.99	0.44-1.80	0.94-1.98	0.07-0.35	1.99-4.32	0.32-0.71	10.31-19.97	81.23-96.24	72.89-94.17	0.50-1.02	81.34-96.47	52.86-71.74	26.29-44.13
	Avg.,	49.33	19.22	10.08	0.07	1.03	0.51	0.31	1.07	1.35	0.22	2.60	0.53	14.81	90.94	85.88	0.76	90.88	61.67	37.40
	STD (±)	5.38	1.64	1.85	0.03	0.48	0.29	0.24	0.37	0.33	0.08	0.48	0.10	2.71	3.49	4.90	0.14	3.48	5.17	3.88
Goa (11)	Range	43.19-56.47	14.81-20.41	6.03-14.47	0.05-0.55	1.23-3.50	0.42-2.35	0.20-0.72	1.08-1.51	1.16-2.10	0.21-0.49	2.46-3.15	0.31-0.86	8.57-14.90	80.13-90.81	74.00-84.87	0.60-1.32	78.79-91.41	47.05-67.95	31.34-42.56
	Avg.,	49.38	17.65	9.66	0.17	2.23	1.06	0.42	1.30	1.59	0.32	2.81	0.56	11.46	86.43	80.05	0.95	84.54	56.52	35.69
	STD (±)	4.23	1.72	2.64	0.18	0.75	0.54	0.14	0.13	0.36	0.08	0.23	0.19	2.12	3.12	3.49	0.22	3.84	6.65	3.26
Archean- Proterozoic Terrain (APT)	Range	34.08-65.74	14.81-26.06	6.03-16.03	0.02-0.55	0.34-3.53	0.07-2.59	0.05-1.89	0.44-2.66	0.74-2.10	0.07-0.80	1.38-4.32	0.31-0.86	8.57-30.65	76.13-96.24	67.23-94.17	0.50-1.32	75.61-96.47	47.05-71.74	26.29-54.21

Preprints.org (www.preprints.org) | NOT PEER-REVIEWED | Posted: 11 October 2024 doi:10.20944/preprints202410.0793.v1

	Avg.,	45.07	20.30	10.80	0.12	1.56	0.80	0.41	1.31	1.36	0.32	2.29	0.54	15.76	88.57	82.75	0.84	87.83	59.17	40.15
	STD (±)	6.93	2.82	2.30	0.10	0.80	0.50	0.29	0.47	0.32	0.14	0.61	0.12	4.53	3.62	14.34	0.17	3.84	4.9	3.72
Maharashtra (21)	Range	46.24-57.94	14.98-22.11	0.81-9.37	0.05-0.37	0.93-5.76	0.47-10.91	0.10-1.67	0.38-1.82	1.07-8.36	0.08-0.60	2.41-3.72	0.04-0.56	1.96-15.77	55.08-92.99	52.15-91.00	0.39-1.45	56.03-89.80	44.10-85.37	22.98-31.62
	Avg.,	53.34	18.06	3.12	0.20	2.55	2.93	0.64	0.78	3.43	0.25	2.99	0.18	6.12	81.02	77.46	0.78	75.96	65.72	28.43
	STD (±)	3.46	2.11	2.45	0.08	1.20	2.25	0.40	0.32	1.49	0.11	0.38	0.15	2.67	8.77	8.73	0.27	9.41	10.54	2.60
Gujarat (17)	Range	50.55-63.44	12.26-16.32	0.30-7.08	0.09-0.24	2.30-3.72	3.03-10.88	0.77-1.91	0.79-1.58	1.59-3.42	0.13-0.33	3.17-4.75	0.02-0.50	4.19-8.81	46.56-77.56	41.06-73.78	0.97-1.87	48.67-75.85	37.37-57.14	18.73-30.73
	Avg.,	55.71	14.17	3.68	0.15	2.93	6.16	1.31	1.25	2.36	0.17	3.97	0.26	6.27	62.20	56.72	1.28	60.58	48.93	24.30
	STD (±)	3.36	1.46	1.62	0.04	0.41	1.86	0.32	0.26	0.53	0.05	0.50	0.12	1.35	7.54	8.09	0.27	6.24	6.17	3.12

Preprints.org (www.preprints.org) | NOT PEER-REVIEWED | Posted: 11 October 2024 doi:10.20944/preprints202410.0793.v1

Deccan Trap Terrain (DTT)	Range	46.63-63.44	12.26-22.11	0.30-9.37	0.05-0.37	0.93-5.76	0.47-10.91	0.10-1.91	0.38-1.82	1.07-8.36	0.08-0.60	2.41-4.75	0.02-0.56	1.96-15.77	46.56-92.99	41.06-91.00	0.39-1.87	48.67-89.80	37.37-85.37	18.73-31.62
	Avg.,	54.40	16.32	3.37	0.17	2.72	4.37	0.94	0.99	2.95	0.22	3.43	0.22	6.19	71.61	67.09	1.03	68.27	57.32	26.36
	STD (±)	3.57	2.67	2.11	0.07	0.94	2.63	0.50	0.38	1.27	0.09	0.66	0.14	2.16	8.15	8.41	0.27	7.82	8.35	2.86
West Coast of India River Average Silt (WCIRAS)	**Range**	**34.08-65.74**	**12.26-26.06**	**0.30-16.03**	**0.34-5.76**	**0.07-10.91**	**0.05-1.91**	**0.38-2.66**	**0.74-8.36**	**0.02-0.55**	**0.07-0.80**	**1.61-4.75**	**0.02-0.86**	**1.96-30.65**	**46.56-96.24**	**41.06-94.17**	**0.39-1.87**	**48.67-96.47**	**37.37-85.37**	**18.73-54.21**
	Avg.,	**49.30**	**18.62**	**7.66**	**2.14**	**2.58**	**0.67**	**1.17**	**2.03**	**0.14**	**0.27**	**2.81**	**0.41**	**1.96-30.65**	**81.79**	**76.86**	**0.89**	**80.24**	**59.03**	**34.63**
	STD (±)	**4.07**	**3.38**	**4.30**	**0.87**	**1.56**	**0.39**	**0.46**	**1.16**	**0.08**	**0.13**	**0.38**	**0.13**	**1.96-30.65**	**5.43**	**12.14**	**0.28**	**12.47**	**8.96**	**3.37**
Reference Sediments	PAAS	62.80	18.90	7.22	0.11	2.20	1.30	1.20	3.70	1.00	0.16	3.32	0.38	18.90	75.29	-	-	63.36	55.92	23.97

	UCC	66.20	15.30	5.57	0.09	2.47	3.57	3.25	2.78	0.63	0.15	4.33	0.36	24.29	61.44	-	-	75.67	47.24	29.37

CIA: Chemical Index of Alteration (Nesbitt and Young 1982); PIA: Plagioclase Index of Alteration (Fedo et al. (1995, 1996); ICV: Index of Chemical Variability (Cox et al. 1995; Cullers 2000);MIA : Mafic Index of Alteration (Oxic) and MIA : Mafic Index of Alteration (Redox) (Babechuk and Fedo (O) (R) 2022); IOL: Index of Laterization (Babechuk and Fedo 2022); APT: Archean- Proterozoic Terrain (this study); DTT: Deccan Trap Terrain (this study); WCIRAC: West Coast of India River Average Clay (this study); WCIRAS: West Coast of India River Average Silt (this study); PASS: Post Archean average Australian Shale (Pourmand et al. 2012); UCC: Upper Continental Crust (Rudnick and Gao 2003).

Table 2. Trace elements content (μg/g) of the clay fraction (<4 μm) of sediments in the rivers of West Coast of India.

State (No. of Rivers)		Sc	V	Cr	Co	Ni	Cu	Zn	Ga	Rb	Sr	Nb	Cs	Ba	Hf	Th	U	Zr	Ta	Pb	Y	La	Ce	Yb
Kerala (21)	Range	20.635 - 32.939	111.228-247.004	108.934-286.565	18.621 - 41.839	42.601 - 101.548	29.208-111.952	29.812 - 155.052	24.975 - 37.808	36.921 - 91.318	45.695 - 160.748	10.997 - 21.144	2.399 - 6.017	169.206-805.442	3.647-6.870	7.098-24.337	1.542 - 5.112	106.617-220.885	0.738 - 1.285	12.152 - 55.830	16.558 - 32.174	29.485 - 95.765	63.296 - 179.624	1.864 - 3.336
	Avg.,	26.541	175.490	158.778	29.480	63.448	73.452	58.064	33.533	61.766	79.312	14.930	3.569	381.114	4.769	11.915	2.569	147.032	0.969	31.707	25.822	55.635	109.026	2.723
	STD ±	3.292	39.857	52.253	7.767	16.006	19.719	30.319	3.588	15.075	29.618	2.811	0.825	199.435	0.851	3.966	1.004	27.292	0.144	11.619	3.762	19.957	36.471	0.380

Karnataka (20)	Range	14.307-36.603	136.105-347.618	82.778-897.427	11.395-55.126	46.310-129.463	76.344-231.775	53.654-195.438	24.545-39.110	31.908-88.767	29.474-71.719	11.333-26.539	3.222-6.995	104.126-288.198	4.027-10.586	7.939-25.704	1.629-6.168	136.561-393.665	1.040-2.388	17.312-51.190	8.572-27.410	8.035-42.580	29.500-86.723	1.238-2.966
	Avg.,	22.491	228.554	203.823	24.735	72.184	133.002	85.446	32.481	61.710	49.209	16.625	4.984	177.673	5.626	13.924	3.917	198.999	1.550	31.859	16.313	24.512	66.322	1.876
	SD (±)	7.090	64.939	168.245	11.363	18.098	48.957	32.997	4.005	17.035	10.621	3.600	1.285	49.698	1.665	4.884	1.133	66.097	0.373	9.974	4.828	9.141	15.286	0.479
Goa (11)	Range	16.044-29.542	178.553-273.344	146.390-237.876	17.483-39.659	57.233-74.550	91.655-194.898	63.406-128.709	23.872-31.193	53.522-87.735	53.389-80.888	12.603-20.291	4.424-7.334	140.514-255.500	4.939-7.866	9.140-15.503	3.513-7.619	175.519-282.745	1.070-1.853	21.798-88.871	16.050-28.522	17.450-37.343	52.803-87.536	1.892-2.748
	Avg.,	24.123	222.571	187.975	30.539	63.886	121.412	84.618	27.003	74.508	70.698	15.604	5.931	185.070	6.142	12.544	4.939	220.424	1.425	34.096	22.733	28.772	71.293	2.333

Preprints.org (www.preprints.org) | NOT PEER-REVIEWED | Posted: 11 October 2024 doi:10.20944/preprints202410.0793.v1

	SD (±)	3.627	31.299	23.421	7.853	5.550	33.427	18.874	2.266	9.906	10.212	2.860	0.908	36.729	0.987	1.887	1.180	37.971	0.241	18.693	4.874	6.236	10.335	0.331
Archean-Proterozoic Terrain (APT)	Range	14.307-36.603	111.228-347.618	82.778-897.427	11.395-55.126	42.601-129.463	29.208-231.775	29.812-195.438	23.872-39.110	31.908-91.318	29.474-160.748	10.997-26.539	2.399-7.334	104.126-805.442	3.647-10.586	7.098-25.704	1.542-7.619	106.617-393.665	0.738-2.388	12.152-88.871	8.572-32.174	8.035-95.765	29.500-179.624	1.238-3.336
	Avg.	24.472	205.859	182.279	27.879	66.901	106.501	74.213	31.747	64.440	65.912	15.725	4.613	261.397	5.389	12.821	3.589	182.544	1.289	32.271	21.511	37.982	84.620	2.315
	SD (±)	5.374	55.028	110.183	9.503	15.695	45.140	31.878	4.291	15.627	24.388	3.180	1.386	163.369	1.345	4.072	1.418	56.012	0.380	12.627	6.121	20.315	32.318	0.555
Maharashtra (21)	Range	26.371-58.580	194.681-465.372	86.186-267.990	27.035-70.839	53.673-104.417	133.713-275.273	64.061-192.930	23.349-45.456	26.920-92.183	42.265-217.870	9.002-18.219	1.670-7.822	128.836-362.785	4.319-9.142	5.400-18.302	1.000-5.902	158.734-321.440	0.904-1.712	8.604-39.252	20.649-54.546	20.087-46.223	45.041-127.803	2.053-3.924

	Avg.	40.147	343.606	159.771	48.828	67.892	204.181	102.430	30.096	49.719	75.981	12.767	4.012	193.895	6.797	8.651	2.692	248.783	1.250	23.460	34.763	28.195	68.631	2.804
	SD (±)	8.210	75.765	46.991	12.268	12.018	47.942	32.047	4.772	19.262	38.998	2.940	1.816	59.513	1.230	3.331	1.377	45.455	0.249	8.440	8.949	6.895	19.883	0.471
Gujarat (17)	Range	27.045-43.052	164.990-424.366	105.933-968.394	28.294-91.345	42.412-536.775	110.882-391.214	52.217-697.892	23.007-30.963	41.537-101.176	83.443-374.887	11.194-15.159	3.449-8.564	163.612-382.990	4.954-7.044	6.817-14.281	1.141-2.444	182.271-270.611	0.966-1.577	11.173-77.110	26.256-32.431	20.980-35.591	47.115-71.305	2.012-2.388
	Avg.	36.241	264.236	172.995	40.262	75.466	165.342	117.304	25.963	65.382	129.261	13.054	5.016	225.596	5.902	8.731	1.583	221.234	1.225	21.669	29.637	26.779	57.510	2.235
	SD (±)	3.927	73.682	205.485	13.683	118.933	66.201	151.432	1.938	15.480	65.978	1.093	1.201	56.848	0.577	1.768	0.329	22.506	0.156	15.569	2.189	3.702	5.571	0.140
Deccan Trap Terrain (DTT)	Ra	26.371	164.990-	86.186-	27.035	42.412	110.882-	52.217	23.007	26.920	42.265	9.002-	1.670	128.836-	4.319-	5.400-	1.000	158.734-	0.904	8.604-	20.649	20.087	45.041	2.012

	nge	-58.580	465.372	968.394	-91.345	-536.775	391.214	-697.892	-45.456	-101.176	-374.887	18.219	-8.564	382.990	9.142	18.302	-5.902	321.440	-1.712	77.110	-54.546	-46.223	-127.803	-3.924
	Avg.,	38.400	308.098	165.687	44.996	71.280	186.805	109.084	28.247	56.726	99.817	12.895	4.461	208.077	6.397	8.687	2.196	236.459	1.239	22.659	32.470	27.561	63.656	2.549
	SD (±)	6.854	83.965	139.632	13.451	78.800	59.335	102.605	4.274	19.144	58.526	2.283	1.632	59.726	1.079	2.711	1.177	39.097	0.210	12.006	7.214	5.669	16.079	0.459
West Coast of India River Average Clay (WCIRAC)	**Range**	**14.307-58.580**	**111.228-465.372**	**82.78-968.394**	**11.395-91.345**	**42.412-536.775**	**29.208-391.214**	**29.812-697.892**	**23.007-45.456**	**26.920-101.176**	**29.474-374.887**	**9.002-26.539**	**1.670-8.564**	**104.126-805.442**	**3.647-10.586**	**5.400-25.704**	**1.000-7.619**	**106.617-393.665**	**0.738-2.388**	**8.604-88.871**	**8.572-54.546**	**8.035-95.765**	**29.500-179.624**	**1.238-3.924**
	Avg.,	**30.353**	**249.027**	**175.274**	**35.106**	**68.750**	**140.407**	**88.936**	**30.269**	**61.183**	**80.227**	**14.530**	**4.549**	**238.884**	**5.814**	**11.076**	**3.001**	**205.308**	**1.268**	**28.212**	**26.138**	**33.582**	**75.768**	**2.414**
	SD (	**9.162**	**85.116**	**123.005**	**14.116**	**52.224**	**64.978**	**72.519**	**4.601**	**17.521**	**45.259**	**3.152**	**1.488**	**132.205**	**1.331**	**4.096**	**1.485**	**56.128**	**0.319**	**13.194**	**8.528**	**16.633**	**28.538**	**0.527**

	±)																							
Reference Sediments	PAAS	15.890	150.000	110.000	23.000	55.000	50.000	85.000	20.000	160.000	200.000	19.000	15.000	650.000	5.000	14.600	3.100	210.000	1.500	20.000	27.310	44.560	88.250	2.040
	UCC	14.000	97.000	92.300	17.300	47.300	27.700	67.000	17.500	82.000	320.000	11.800	4.100	624.000	5.260	10.100	2.630	193.000	0.880	17.000	21.000	31.400	63.400	3.012

State (No. of Rivers)		**∑TE**	**Th/Sc**	**Zr/Sc**	**Cr/V**	**Y/Ni**	**Co/Th**	**La/Sc**	**Zr/Co**	**La/Th**	**Th/Yb**	**Th/U**	**Rb/Sr**	**K_2O/Rb**	**Cr/Th**	**Cr/Ni**	**V/Th**
Kerala (21)	Range	991.581-1802.551	0.238-0.944	3.854-9.731	0.694-1.382	0.214-0.669	1.057-5.895	0.955-3.918	2.686-9.095	3.026-10.488	2.210-8.020	2.444-12.313	0.368-1.586	0.061-0.011	5.747-36.894	1.985-3.114	6.537-31.275
	Avg.,	1358.438	0.458	5.622	0.905	0.429	2.763	2.141	5.357	4.813	4.453	5.242	0.868	0.021	14.947	2.485	16.304
	STD ±	212.296	0.167	1.299	0.183	0.116	1.285	0.833	1.798	1.704	1.512	2.614	0.347	0.013	7.901	0.330	6.827
Karnataka (20)	Range	1097.931-2027.128	0.222-1.473	4.235-1.288	0.426-3.350	0.099-0.350	0.443-4.207	0.281-2.388	3.576-23.381	0.751-2.515	3.562-20.755	1.937-7.176	0.725-2.038	0.015-0.022	3.220-110.234	1.787-6.932	5.747-33.781

	Avg.	1368.793	0.694	9.327	0.907	0.234	1.967	1.230	9.450	1.773	8.061	3.685	1.281	0.018	17.981	2.633	18.567
	STD ±	218.062	0.345	3.215	0.619	0.071	1.021	0.633	5.100	0.370	4.177	1.178	0.373	0	22.360	1.070	8.419
Goa (11)	Range	1269.836-1611.232	0.343-0.849	6.544-17.623	0.708-1.075	0.222-0.455	1.145-4.033	0.747-1.640	4.426-15.098	1.281-2.890	4.400-7.200	2.035-3.118	0.892-1.267	0.016 -0.27	9.588-23.105	2.558-4.004	13.407-29.906
	Avg.	1393.509	0.538	9.557	0.856	0.360	2.534	1.198	8.034	2.316	5.450	2.599	1.063	0.020	15.432	2.954	18.200
	SD (±)	92.542	0.150	3.345	0.138	0.087	0.899	0.224	3.709	0.483	0.988	0.366	0.129	0	3.643	0.405	4.533
Archean- Proterozoic Terrain (APT)	Range	991.581-2027.128	0.222-1.473	3.854-17.623	0.426-3.350	0.099-0.669	0.443-5.895	0.281-3.918	2.686-23.381	0.751-10.488	2.210-20.755	1.937-12.313	0.368-2.038	0.015 -0.27	3.220-110.234	1.787-6.932	5.747-33.781
	Avg.	1369.840	0.566	7.879	0.896	0.339	2.409	1.591	7.498	3.116	6.052	4.084	1.068	0.02	16.217	2.641	17.576
	SD (±)	192.985	0.267	3.199	0.400	0.128	1.152	0.800	4.135	1.807	3.210	2.077	0.370	0	14.675	0.730	7.060

Preprints.org (www.preprints.org) | NOT PEER-REVIEWED | Posted: 11 October 2024 doi:10.20944/preprints202410.0793.v1

Maharashtra (21)	Range	1360.433-1980.545	0.112-0.675	4.300-10.757	0.234-0.733	0.292-0.777	1.886-10.900	0.451-1.706	3.204-11.738	2.008-4.673	1.656-7.349	1.882-5.399	0.283-2.026	0.011-0.026	9.134-47.415	1.399-3.610	15.624-72.531
	Avg.,	1624.956	0.239	6.370	0.487	0.520	6.413	0.745	5.472	3.477	3.232	3.610	0.768	0.019	20.820	2.347	44.275
	SD (±)	164.494	0.153	1.521	0.164	0.130	2.809	0.312	2.127	0.873	1.567	1.054	0.481	0	10.617	0.513	16.835
Gujarat (17)	Range	1248.288-3733.648	0.167-0.528	5.301-6.740	0.289-3.060	0.059-0.721	1.981-12.389	0.522-1.316	2.062-7.237	2.492-3.374	2.997-6.809	4.332-6.287	0.192-0.766	0.015-0.02	10.308-131.344	1.804-3.170	11.553-55.574
	Avg.,	1596.461	0.248	6.124	0.652	0.603	4.852	0.756	5.817	3.099	3.931	5.546	0.550	0.02	21.333	2.592	32.199
	SD (±)	565.617	0.083	0.423	0.634	0.159	2.166	0.187	1.099	0.234	0.918	0.493	0.139	0	28.535	0.285	13.035
Deccan Trap Terrain (DTT)	Range	1248.288-3733.648	0.112-0.675	4.300-10.757	0.234-3.060	0.059-0.777	1.886-12.389	0.451-1.706	2.062-11.738	2.008-4.673	1.656-7.349	1.882-6.287	0.192-2.026	0.011-0.026	9.134-131.344	1.399-3.610	11.553-72.531
	Avg.,	1612.208	0.243	6.260	0.561	0.557	5.715	0.750	5.626	3.308	3.545	4.476	0.670	0.02	21.050	2.456	38.873

	SD (±)	391.379	0.125	1.159	0.442	0.148	2.629	0.260	1.732	0.687	1.348	1.287	0.382	0	20.325	0.439	16.239
West Coast of India River Average Clay (WCIRAC)	**Range**	**991.581-3734.378**	**0.112-1.473**	**3.854-17.623**	**0.234-3.350**	**0.059-0.777**	**0.443-12.389**	**0.281-3.918**	**2.062-23.381**	**0.751-10.488**	**1.656-20.755**	**1.882-12.313**	**0.192-2.038**	**0.011-0.061**	**3.220-131.344**	**1.399-6.932**	**5.747-72.531**
	Avg.,	**1473.054**	**0.429**	**7.196**	**0.754**	**0.431**	**3.805**	**1.236**	**6.707**	**3.197**	**4.993**	**4.249**	**0.900**	**0.019**	**18.257**	**2.563**	**26.568**
	SD (±)	**315.457**	**0.270**	**2.659**	**0.448**	**0.174**	**2.516**	**0.755**	**3.451**	**1.441**	**2.865**	**1.788**	**0.422**	**0.007**	**17.347**	**0.627**	**15.814**
Reference Sediments	PAAS	1807.090	0.919	13.216	0.733	0.497	1.575	2.804	9.130	3.052	7.157	4.710	0.800	-	7.534	2.000	10.274
	UCC	1650.870	0.721	13.786	0.952	0.444	1.713	2.243	11.156	3.109	3.353	3.840	0.256	-	9.139	1.951	9.604

APT: Archean- Proterozoic Terrain (this study); DTT: Deccan Trap Terrain (this study); WCIRAC: West Coast of India River Average Clay (this study); PASS: Post Archean average Australian Shale (Pourmand et al. 2012); UCC: Upper Continental Crust (Rudnick and Gao 2003).

Table 3. Trace elements content (μg/g) of the silt fraction (>4 to 63 μm) of sediments in the rivers of West Coast of India.

State (No. of Rivers)		Sc	V	Cr	Co	Ni	Cu	Zn	Ga	Rb	Sr	Nb	Cs	Ba	Hf	Th	U	Zr	Ta	Pb	Y	La	Ce	Yb
Kerala (21)	Ra	14.854-	97.664-	118.321-	15.536-	35.917-	31.873-	57.813-	18.208-	26.992-	61.447-	11.153-	1.098-	186.306-	5.498-	6.937-	1.260-	188.075-	0.602-	19.125-	19.013-	44.164-	88.862-	2.077-

	nge	29.272	254.562	350.871	43.836	90.855	94.864	262.672	47.222	90.741	337.381	34.864	2.939	1503.009	65.310	116.474	14.628	2435.706	2.586	87.628	38.583	232.437	521.220	4.319
	Avg.,	24.274	181.089	174.381	29.602	56.458	68.216	148.772	33.527	59.268	155.883	20.47	2.197	642.236	18.707	30.731	3.924	646.91	1.278	41.001	30.508	105.36	201.265	3.102
	STD±	3.966	45.163	76.903	7.459	15.724	17.486	67.617	6.186	20.956	79.156	6.357	0.491	401.360	15.033	27.443	3.266	538.363	0.515	18.694	5.379	56.695	111.539	0.542
Karnataka (20)	Range	11.307-39.132	104.966-536.010	80.641-2350.397	10.733-35.554	35.120-146.151	50.123-185.463	44.007-98.212	11.628-39.139	15.114-79.790	36.624-101.549	10.205-23.313	1.663-4.702	98.824-290.563	5.396-27.486	6.273-28.434	1.958-7.147	194.577-1237.728	1.149-2.318	12.945-42.775	13.629-33.747	15.873-72.912	32.635-132.219	1.500-3.904
	Avg.,	22.533	228.920	296.124	21.222	63.728	106.649	67.097	29.130	40.539	61.829	16.905	2.966	194.489	10.917	14.313	4.144	426.758	1.724	25.186	21.573	32.060	68.186	2.400
	SD(±)	8.351	101.912	489.514	6.118	23.302	37.276	15.695	6.645	17.396	18.348	3.206	0.987	49.969	4.850	5.978	1.431	234.761	0.297	7.821	5.284	13.155	23.493	0.598
Goa (11)	Ra	18.965-	183.738-	185.497-	16.628-	44.343-	85.387-	51.774-	16.935-	28.959-	52.106-	13.638-	2.449-	102.865-	6.269-	4.339-	4.006-	229.788-	1.355-	19.446-	18.004-	16.758-	31.783-	2.109-

	nge	28.718	348.378	245.622	39.026	68.937	166.157	73.844	26.490	58.617	107.487	25.627	5.297	274.009	13.274	16.796	7.936	502.269	4.114	57.531	31.954	39.641	89.493	3.339
	Avg.,	22.988	242.942	211.087	28.098	58.584	108.900	63.520	22.547	47.641	84.841	17.556	3.851	203.644	8.724	10.843	5.304	326.408	2.059	29.866	27.507	28.408	61.807	2.767
	SD (±)	2.904	49.259	18.595	7.025	6.884	28.239	7.531	2.669	9.228	17.140	3.831	0.982	50.619	2.255	3.268	1.273	88.031	0.811	11.116	4.796	6.400	16.244	0.343
Archean-Proterozoic Terrain (APT)	Range	11.307-39.132	97.664-536.010	80.641-2350.397	10.733-43.836	35.120-146.151	31.873-185.463	44.007-262.672	11.628-47.222	15.114-90.741	36.624-337.381	10.205-34.864	1.098-5.297	98.824-1503.009	5.396-65.310	4.339-116.474	1.260-14.628	188.075-2435.706	0.602-4.114	12.945-87.628	13.629-38.583	15.873-232.437	31.783-521.220	1.500-4.319
	Avg.,	23.333	212.570	228.970	26.061	59.704	91.605	99.325	29.513	49.605	104.681	18.483	2.843	377.247	13.599	20.210	4.301	494.438	1.615	32.563	26.437	60.889	120.580	2.761
	SD (±)	5.869	76.530	307.772	7.790	17.875	34.241	59.887	7.072	19.318	67.266	5.034	1.022	336.330	10.820	19.720	2.356	391.371	0.600	15.372	6.528	51.970	98.176	0.609
Maharashtra (21)	Ra	18.191-	179.812-	124.634-	25.650-	42.067-	84.521-	46.005-	19.139-	12.762-	50.559-	11.850-	0.533-	83.550-	5.153-	2.628-	0.831-	195.087-	0.900-	7.031-	21.641-	12.698-	29.291-	2.264-

Preprints.org (www.preprints.org) | NOT PEER-REVIEWED | Posted: 11 October 2024 doi:10.20944/preprints202410.0793.v1

	nge	54.444	1308.249	576.092	82.147	103.186	424.443	156.513	39.997	60.436	380.447	68.140	5.174	340.665	21.472	15.640	5.563	1119.754	7.484	38.443	40.056	40.812	98.563	3.656
	Avg.,	37.241	599.333	219.288	54.569	65.729	229.672	88.680	27.206	28.016	114.670	23.684	1.961	176.599	9.627	7.461	2.472	397.791	2.384	18.591	31.774	25.036	56.908	2.984
	SD (±)	10.175	276.646	125.908	13.816	11.951	91.615	30.578	6.011	13.303	68.844	12.209	1.222	70.630	3.974	3.612	1.421	222.874	1.410	8.286	4.977	6.928	17.660	0.464
Gujarat (17)	Range	15.154-28.242	165.008-403.659	77.848-732.654	21.726-66.599	31.267-440.134	81.248-264.516	37.103-387.413	15.974-21.982	30.362-67.086	127.084-340.740	13.123-23.777	1.274-4.381	166.051-323.900	4.848-9.071	6.667-24.500	1.283-3.241	179.656-353.630	0.853-2.127	10.548-51.997	26.210-38.237	22.815-53.570	47.952-103.572	2.299-3.514
	Avg.,	20.393	280.239	153.228	34.949	62.746	130.616	72.733	18.324	45.902	189.427	18.446	2.602	238.464	6.713	11.423	1.965	250.858	1.559	17.292	31.146	32.941	67.287	2.821
	SD (±)	3.541	73.025	153.310	9.933	97.386	40.970	82.149	2.026	11.312	52.791	3.085	0.825	39.802	1.118	4.358	0.547	45.837	0.329	9.767	3.190	7.955	14.942	0.300
Deccan Trap Terrain (DTT)	Ra	15.154-	165.008-	77.848-	21.726-	31.267-	81.248-	37.103-	15.974-	12.762-	50.559-	11.850-	0.533-	83.550-	4.848-	2.628-	0.831-	179.656-	0.853-	7.031-	21.641-	12.698-	29.291-	2.264-

	nge	54.444	1308.249	732.654	82.147	440.134	424.443	387.413	39.997	67.086	380.447	68.140	5.174	340.665	21.472	24.500	5.563	1119.754	7.484	51.997	40.056	53.570	103.572	3.656
	Avg.,	29.704	456.580	189.735	45.792	64.394	185.357	81.546	23.233	36.018	148.114	21.341	2.248	204.275	8.324	9.234	2.245	332.058	2.015	18.010	31.493	28.572	61.551	2.911
	SD (±)	11.552	263.683	140.858	15.607	64.658	88.058	59.061	6.430	15.239	72.014	9.574	1.098	65.980	3.352	4.388	1.134	182.320	1.137	8.876	4.230	8.317	17.102	0.403
West Coast of India River Average Silt (WCIRAS)	**Range**	**11.307-54.444**	**97.664-1308.249**	**77.848-2350.397**	**10.733-82.147**	**31.267-440.134**	**31.873-424.443**	**37.103-387.413**	**11.628-47.222**	**12.762-90.741**	**36.624-380.447**	**10.205-68.140**	**0.533-5.297**	**83.550-1503.009**	**4.848-65.310**	**2.628-116.474**	**0.931-14.628**	**179.656-1435.706**	**0.602-7.484**	**7.031-87.628**	**13.629-40.056**	**12.698-232.437**	**29.291-521.220**	**1.500-4.319**
	Avg.,	**26.023**	**315.597**	**212.404**	**34.392**	**61.684**	**131.189**	**91.818**	**26.862**	**43.868**	**123.019**	**19.689**	**2.591**	**304.215**	**11.372**	**15.575**	**3.433**	**425.877**	**1.784**	**26.418**	**28.572**	**47.245**	**95.657**	**2.824**
	SD (±)	**9.232**	**216.679**	**250.815**	**15.234**	**43.892**	**77.870**	**59.861**	**7.455**	**18.866**	**72.209**	**7.392**	**1.089**	**272.050**	**8.867**	**16.142**	**2.181**	**328.779**	**0.885**	**14.846**	**6.177**	**42.826**	**80.649**	**0.534**

Reference Sediments	PAAS	15.890	150.000	110.000	23.000	55.000	50.000	85.000	20.000	160.000	200.000	19.000	15.000	650.000	5.000	14.600	3.100	210.000	1.500	20.000	27.310	44.560	88.250	2.040
	UCC	14.000	97.000	92.300	17.300	47.300	27.700	67.000	17.500	82.000	320.000	11.800	4.100	624.000	5.260	10.100	2.630	193.000	0.880	17.000	21.000	31.400	63.400	3.012

State (No. of Rivers)		**∑TE**	**Th/Sc**	**Zr/Sc**	**Cr/V**	**Y/Ni**	**Co/Th**	**La/Sc**	**Zr/Co**	**La/Th**	**Th/Yb**	**Th/U**	**Rb/Sr**	**K_2O/Rb**	**Cr/Th**	**Cr/Ni**	**V/Th**
Kerala (21)	Range	1395.114-3848.586	0.237-5.317	8.226-111.194	0.716-1.486	0.273-0.929	0.201-6.296	1.509-10.611	5.993-103.999	1.999-6.759	1.807-31.859	2.761-18.264	0.188-1.357	0.017-0.037	1.016-46.171	2.037-4.897	1.083-36.290
	Avg.,	2338.935	1.266	26.650	0.963	0.540	0.963	4.340	21.853	3.428	9.907	7.830	0.380	0.027	5.674	3.089	5.893
	STD ±	601.675	1.313	26.082	0.228	0.182	1.655	2.666	27.469	1.562	7.533	4.794	0.312	0.000	11.988	0.687	9.802
Karnataka (20)	Range	1148.902-3826.032	0.245-1.640	5.677-71.398	0.340-6.734	0.183-0.637	0.435-4.673	0.433-4.206	5.473-79.219	1.158-3.188	2.613-16.469	1.901-7.526	0.327-1.323	0.021-0.046	3.265-236.694	1.684-16.082	5.939-39.056
	Avg.,	1635.173	0.726	21.896	1.201	0.360	1.810	1.644	22.342	2.320	6.513	3.596	0.670	0.028	25.725	3.768	18.940
	STD ±	600.637	0.406	15.322	1.344	0.109	1.069	0.897	16.141	0.538	3.770	1.456	0.265	0.000	50.132	3.013	11.365

Preprints.org (www.preprints.org) | NOT PEER-REVIEWED | Posted: 11 October 2024 doi:10.20944/preprints202410.0793.v1

Goa (11)	Range	1319.378-1753.873	0.205-0.676	9.674-21.269	0.599-1.114	0.299-0.594	1.260-8.085	0.792-1.787	6.925-23.738	1.945-3.862	1.855-5.206	1.043-3.160	0.398-0.706	0.021-0.037	12.991-53.113	3.045-4.921	15.717-62.361
	Avg.,	1499.403	0.477	14.446	0.895	0.476	3.041	1.238	12.713	2.742	3.901	2.063	0.568	0.028	22.019	3.660	25.559
	SD (±)	144.137	0.151	4.449	0.160	0.097	1.925	0.260	5.906	0.597	1.031	0.546	0.087	0.000	10.976	0.640	14.060
Archean- Proterozoic Terrain (APT)	Range	1148.902-3848.586	0.205-5.317	5.677-111.194	0.340-6.734	0.183-0.929	0.201-8.085	0.433-10.611	5.473-103.999	1.158-6.759	1.807-31.859	1.043-18.264	0.188-1.357	0.017-0.046	1.016-236.694	1.684-16.082	1.083-62.361
	Avg.,	1890.664	0.930	22.863	1.034	0.473	2.101	2.728	21.722	3.243	7.172	5.217	0.569	0.027	19.265	3.455	17.318
	SD (±)	649.463	0.938	19.633	0.846	0.170	1.572	2.322	20.603	1.435	5.700	4.152	0.271	0.000	32.527	1.940	12.425
Maharashtra (21)	Range	1483.292-3738.619	0.065-0.660	5.900-28.979	0.132-1.228	0.254-0.588	2.280-24.939	0.316-1.723	3.265-18.511	2.359-5.671	1.007-4.969	1.627-6.194	0.066-0.950	0.020-0.043	10.223-96.157	2.045-9.173	15.985-253.897
	Avg.,	2104.976	0.230	11.317	0.460	0.492	9.624	0.750	7.822	3.726	2.526	3.398	0.313	0.029	35.782	3.299	105.718
	SD (±)	483.883	0.164	6.685	0.345	0.077	5.865	0.375	4.775	0.951	1.199	1.326	0.242	0.000	23.824	1.681	75.202
Gujarat (17)	Range	1081.086-2897.201	0.304-1.447	7.658-20.749	0.300-2.770	0.068-1.117	0.887-6.919	1.008-3.164	3.034-12.901	2.187-3.459	2.776-7.645	4.907-7.705	0.135-0.456	0.019-0.034	4.544-76.118	1.665-5.744	6.735-48.798

	Avg.,	1557.880	0.589	12.693	0.563	0.767	3.452	1.680	7.641	2.991	3.990	5.722	0.255	0.028	14.745	2.913	27.158
	SD (±)	381.926	0.291	3.432	0.576	0.224	1.448	0.582	2.327	0.329	1.205	0.708	0.082	0.000	16.133	0.859	10.031
Deccan Trap Terrain (DTT)	Range	1081.086 - 3738.619	0.065 - 1.447	5.900-28.979	0.132 - 2.770	0.068 - 1.117	0.887-24.939	0.316-3.164	3.034-18.511	2.187 - 5.671	1.007-7.645	1.627-7.705	0.066 -0.95	0.019 - 0.043	4.544-96.157	1.665-9.173	6.735-253.897
	Avg.,	1860.223	0.391	11.932	0.506	0.615	6.863	1.166	7.741	3.397	3.181	4.437	0.287	0.028	26.371	3.126	70.573
	SD (±)	515.404	0.290	5.453	0.459	0.210	5.401	0.665	3.831	0.820	1.396	1.593	0.188	0.000	23.059	1.373	68.319
West Coast of India River Average Silt (WCIRAS)	**Range**	**1082.666 - 3848.586**	**0.065 - 5.317**	**5.677-111.194**	**0.132 - 6.734**	**0.068 - 1.117**	**0.201-24.939**	**0.316-10.611**	**3.034-103.999**	**1.158 - 6.759**	**1.007-31.859**	**1.043-18.264**	**0.066 - 1.357**	**0.017 - 0.046**	**1.016-236.694**	**1.665-16.082**	**1.083-253.897**
	Avg.,	**1878.625**	**0.702**	**18.248**	**0.811**	**0.533**	**4.111**	**2.068**	**15.819**	**3.308**	**5.486**	**4.888**	**0.450**	**0.028**	**22.265**	**3.316**	**39.803**
	SD (±)	**593.281**	**0.782**	**16.209**	**0.753**	**0.200**	**4.375**	**1.969**	**17.250**	**1.211**	**4.833**	**3.329**	**0.277**	**0.005**	**28.979**	**1.722**	**52.236**
Reference Sediments	PAAS	1807.090	0.919	13.216	0.733	0.497	1.575	2.804	9.130	3.052	7.157	4.710	0.800	-	7.534	2.000	10.274
	UCC	1650.870	0.721	13.786	0.952	0.444	1.713	2.243	11.156	3.109	3.353	3.840	0.256	-	9.139	1.951	9.604

APT: Archean- Proterozoic Terrain (this study); DTT: Deccan Trap Terrain (this study); WCIRAS: West Coast of India River Average Silt (this study); PASS: Post Archean average Australian Shale (Pourmand et al. 2012); UCC: Upper Continental Crust (Rudnick and Gao 2003).

Table 4. Correlation matrix (APT- Archean- Proterozoic Terrain; DTT- Deccan Trap Terrain).

Preprints.org (www.preprints.org) | NOT PEER-REVIEWED | Posted: 11 October 2024 doi:10.20944/preprints202410.0793.v1

APTDTT	**SiO_2**	**Al_2O_3**	**Fe_2O_3**	**MnO**	**MgO**	**CaO**	**Na_2O**	**K_2O**	**TiO_2**	**P_2O_5**	**ΣREE**	**Y**	**La**	**Ce**	**Yb**	**Zr**	**Hf**	**U**	**Th**	**Sc**	**V**	**Cr**	**Co**	**Ni**	**Cu**	**Zn**	**Ga**	**Rb**	**Sr**	**Nb**	**Cs**	**Ba**	**Ta**	**Pb**
SiO_2	1	-0.27	**-0.57**	-0.07	0.18	0.43	**-0.58**	0.08	0.06	-0.38	**-0.50**	-0.15	-0.41	**-0.50**	-0.45	0.03	0.01	**-0.61**	-0.28	0.01	-0.20	0.01	-0.15	-0.01	-0.37	0.01	-0.37	0.04	0.26	-0.11	-0.04	0.14	-0.26	-0.20
Al_2O_3	-0.39	1	-0.02	-0.21	**-0.53**	**-0.60**	-0.18	-0.28	0.45	**0.50**	0.09	-0.19	-0.03	0.28	0.24	**0.54**	**0.59**	**0.67**	0.28	-0.01	0.34	-0.16	-0.21	-0.09	0.22	-0.11	**0.68**	-0.04	-0.31	**0.54**	0.11	-0.31	**0.60**	0.20
Fe_2O_3	-0.31	-0.04	1	0.24	-0.18	-0.39	0.15	0.02	-0.39	0.14	**0.64**	0.22	**0.51**	**0.64**	0.36	-0.18	-0.17	**0.50**	0.34	0.06	0.15	0.16	0.40	0.13	0.30	0.10	0.26	0.03	-0.38	-0.12	0.06	0.13	0.03	0.23
MnO	-0.19	-0.12	0.32	1	-0.10	-0.05	-0.12	-0.29	-0.08	0.31	0.28	**0.68**	0.17	0.03	**0.57**	-0.01	-0.01	-0.29	-0.33	0.42	0.20	0.21	**0.66**	0.21	0.40	0.23	-0.12	-0.46	-0.20	-0.47	-0.44	0.38	-0.28	0.15
MgO	-0.21	-0.28	0.02	0.36	1	**0.65**	-0.14	**0.52**	-0.27	-0.33	-0.24	-0.11	-0.02	-0.35	-0.43	-0.44	-0.44	-0.38	-0.18	-0.27	**-0.61**	-0.08	-0.28	-0.11	-0.33	-0.03	**-0.66**	0.19	0.44	-0.28	0.05	-0.06	-0.30	-0.21
CaO	-0.29	-0.45	-0.06	0.13	**0.50**	1	-0.18	**0.58**	-0.23	-0.34	-0.30	-0.17	-0.07	-0.38	**-0.52**	-0.40	-0.45	**-0.56**	-0.10	-0.23	**-0.57**	-0.12	-0.33	-0.14	-0.41	-0.12	**-0.63**	0.31	**0.77**	-0.16	0.18	0.34	-0.17	-0.27

Na_2O	-0.20	**-0.50**	-0.28	-0.15	0.17	**0.71**	1	-0.06	-0.11	-0.10	0.13	0.10	0.14	0.09	0.23	-0.12	-0.14	0.12	0.00	0.08	0.08	-0.06	0.02	-0.05	0.12	-0.09	0.10	-0.05	-0.12	-0.06	-0.05	-0.17	-0.09	-0.11
K_2O	-0.10	**-0.63**	-0.24	0.11	**0.53**	**0.62**	**0.75**	1	-0.35	-0.12	0.12	-0.40	0.33	0.19	**-0.52**	-0.45	-0.47	0.09	**0.50**	**-0.58**	**-0.74**	-0.25	-0.47	-0.25	-0.36	-0.17	-0.28	**0.83**	0.47	0.31	**0.72**	0.14	0.26	-0.01
TiO_2	0.37	-0.05	-0.05	-0.25	0.00	-0.14	-0.08	-0.02	1	0.33	-0.30	-0.06	-0.42	-0.20	0.15	**0.70**	**0.70**	0.06	-0.18	0.22	**0.61**	-0.11	-0.13	-0.05	0.07	-0.08	**0.50**	-0.36	-0.43	0.44	-0.24	-0.19	0.38	-0.05
P_2O_5	**-0.67**	0.34	0.15	0.23	0.17	0.11	-0.05	-0.04	-0.16	1	0.24	0.17	0.18	0.25	0.40	0.20	0.25	0.36	0.23	-0.03	0.18	0.18	0.21	0.24	**0.61**	0.30	0.28	-0.08	-0.34	0.27	0.01	0.13	0.41	**0.58**
ΣREE	**-0.64**	0.43	-0.02	0.23	0.06	0.15	-0.02	-0.02	-0.15	**0.79**	1	0.35	**0.92**	**0.91**	0.46	-0.33	-0.32	**0.51**	**0.57**	-0.06	-0.01	-0.05	0.21	-0.09	0.11	-0.09	0.23	0.16	-0.26	0.09	0.10	-0.02	0.25	0.12
Y	**-0.71**	0.31	0.26	0.41	0.21	0.22	-0.01	0.00	-0.28	**0.58**	**0.70**	1	0.14	-0.02	**0.84**	0.18	0.18	-0.33	**-0.50**	**0.71**	0.30	0.07	**0.66**	0.06	0.41	0.12	-0.08	**-0.65**	-0.23	**-0.62**	**-0.68**	-0.02	-0.46	-0.19
La	**-0.62**	0.46	-0.08	0.19	0.03	0.13	-0.01	-0.02	-0.12	**0.76**	**0.99**	**0.66**	1	**0.84**	0.19	**-0.60**	**-0.58**	0.43	**0.69**	-0.31	-0.30	-0.02	0.02	-0.09	-0.06	-0.09	0.01	0.39	-0.08	0.13	0.27	0.08	0.27	0.15
Ce	**-0.58**	0.41	-0.01	0.21	0.01	0.10	-0.07	-0.03	-0.15	**0.77**	**0.98**	**0.62**	**0.95**	1	0.21	-0.26	-0.26	**0.75**	**0.79**	-0.27	0.03	-0.06	0.04	-0.09	0.04	-0.12	0.43	0.37	-0.28	0.40	0.36	-0.02	**0.50**	0.25

Preprints.org (www.preprints.org) | NOT PEER-REVIEWED | Posted: 11 October 2024 doi:10.20944/preprints202410.0793.v1

Yb	**-0.71**	0.39	0.25	0.32	0.08	0.16	0.01	-0.08	-0.20	0.47	**0.59**	**0.94**	**0.55**	**0.50**	1	0.39	0.42	0.10	-0.26	**0.65**	**0.50**	0.01	**0.57**	0.03	**0.53**	0.04	0.30	**-0.63**	-0.48	-0.29	**-0.57**	-0.16	-0.11	-0.06
Zr	0.40	-0.29	0.05	-0.15	0.05	-0.10	-0.07	0.09	**0.53**	-0.39	**-0.52**	-0.28	**-0.52**	**-0.52**	-0.16	1	**0.99**	0.07	-0.37	**0.53**	**0.68**	-0.24	0.07	-0.14	0.25	-0.16	**0.59**	-0.45	-0.39	0.22	-0.26	-0.23	0.21	-0.20
Hf	0.31	-0.23	0.02	-0.15	0.07	-0.05	-0.03	0.09	**0.56**	-0.33	-0.44	-0.21	-0.44	-0.45	-0.07	**0.98**	1	0.09	-0.36	**0.50**	**0.65**	-0.23	0.06	-0.14	0.26	-0.15	**0.56**	**-0.50**	-0.42	0.20	-0.29	-0.27	0.21	-0.17
U	0.41	-0.48	0.00	-0.13	0.15	-0.09	0.01	0.31	0.15	-0.43	-0.46	-0.26	-0.43	-0.43	-0.34	**0.53**	0.44	1	**0.70**	-0.34	0.13	-0.08	-0.19	-0.04	0.19	-0.07	**0.65**	0.34	-0.32	**0.61**	0.44	-0.23	**0.65**	0.36
Th	0.20	0.03	-0.13	-0.07	-0.23	-0.21	-0.17	0.00	0.27	-0.04	0.18	-0.16	0.25	0.25	-0.23	-0.01	-0.05	0.31	1	**-0.67**	-0.28	-0.09	-0.35	-0.11	-0.15	-0.13	0.25	**0.77**	-0.05	**0.70**	**0.74**	0.13	**0.72**	0.36
Sc	-0.33	0.15	0.27	0.18	-0.01	0.11	0.06	-0.15	0.14	0.06	0.15	0.46	0.11	0.07	**0.62**	0.01	0.11	-0.45	-0.38	1	**0.60**	-0.06	0.44	-0.05	0.30	-0.06	0.29	**-0.74**	-0.26	**-0.51**	**-0.69**	-0.06	-0.44	-0.40
V	0.23	-0.33	**0.50**	-0.04	-0.21	-0.06	-0.03	-0.10	0.40	-0.32	-0.43	-0.16	**-0.50**	-0.40	-0.01	**0.55**	**0.54**	0.05	-0.19	0.48	1	0.11	0.41	0.12	0.35	0.04	**0.66**	**-0.63**	**-0.60**	0.07	-0.45	0.03	0.09	-0.01
Cr	0.21	-0.13	0.10	-0.08	-0.13	0.04	-0.02	-0.18	0.09	-0.22	-0.25	-0.08	-0.32	-0.21	-0.01	0.03	0.09	-0.16	-0.27	0.37	0.34	1	**0.67**	**0.98**	**0.56**	**0.94**	-0.17	-0.16	-0.13	-0.19	-0.13	0.17	-0.22	**0.73**

Co	-0.46	-0.14	**0.60**	**0.50**	0.28	0.30	0.05	0.17	-0.22	0.28	0.24	**0.56**	0.16	0.21	**0.52**	-0.10	-0.07	-0.19	-0.28	0.48	0.39	-0.01	1	**0.66**	**0.66**	**0.65**	-0.03	**-0.51**	-0.32	-0.45	-0.46	0.18	-0.38	0.41
Ni	0.08	-0.14	0.27	-0.09	-0.20	0.02	-0.01	-0.21	0.05	-0.21	-0.33	-0.15	-0.40	-0.31	-0.05	0.05	0.10	-0.22	-0.32	0.40	**0.55**	**0.78**	0.23	1	**0.63**	**0.96**	-0.12	-0.16	-0.13	-0.14	-0.11	0.11	-0.17	**0.75**
Cu	0.32	-0.38	0.42	-0.05	-0.12	-0.09	-0.11	-0.12	0.05	-0.34	**-0.53**	-0.24	**-0.57**	**-0.50**	-0.18	0.30	0.21	0.11	-0.19	0.22	**0.69**	0.22	0.29	0.37	1	**0.68**	0.23	-0.34	-0.38	-0.12	-0.19	0.08	-0.01	**0.61**
Zn	0.40	-0.29	-0.07	-0.12	-0.10	-0.11	0.12	0.12	-0.05	-0.28	-0.39	-0.34	-0.35	-0.38	-0.40	-0.03	-0.15	0.36	0.08	-0.35	-0.03	0.01	-0.24	-0.05	0.31	1	-0.18	-0.14	-0.10	-0.17	-0.10	0.09	-0.20	**0.78**
Ga	-0.04	**0.56**	-0.23	-0.28	**-0.75**	-0.38	-0.20	**-0.51**	0.07	0.23	0.39	0.03	0.41	0.43	0.12	-0.28	-0.24	-0.47	0.33	0.11	-0.05	0.10	-0.24	0.11	-0.17	-0.12	1	-0.06	**-0.51**	**0.52**	0.13	-0.16	**0.52**	0.05
Rb	-0.10	-0.05	0.04	0.28	0.33	-0.05	-0.19	0.37	-0.04	0.07	0.17	0.24	0.17	0.19	0.10	0.02	-0.06	0.41	0.36	-0.25	-0.27	-0.36	0.11	-0.41	-0.13	0.07	-0.27	1	0.34	**0.59**	**0.95**	0.19	**0.50**	0.18
Sr	-0.45	0.07	-0.03	0.28	0.51	0.40	0.11	0.25	0.01	**0.68**	**0.71**	**0.50**	**0.68**	**0.67**	0.35	-0.23	-0.16	-0.22	-0.15	0.02	-0.36	-0.21	0.23	-0.27	-0.44	-0.30	-0.11	0.12	1	-0.15	0.25	0.14	-0.15	-0.18
Nb	0.31	-0.06	-0.19	-0.30	-0.35	-0.17	-0.07	-0.04	**0.64**	-0.06	0.10	-0.27	0.14	0.15	-0.25	0.24	0.25	0.19	**0.72**	-0.19	0.13	-0.06	-0.34	-0.04	-0.15	-0.11	0.44	0.04	-0.04	1	**0.69**	-0.03	**0.91**	0.25

Cs	0.28	-0.48	0.25	0.07	0.20	-0.04	-0.07	0.32	0.25	-0.39	-0.46	-0.18	-0.46	-0.43	-0.23	0.45	0.36	**0.75**	0.28	-0.20	0.28	-0.05	0.08	0.06	0.28	0.29	-0.46	**0.61**	**0.61**	0.22	1	0.21	**0.62**	0.25
Ba	**-0.54**	0.40	0.03	0.21	0.04	0.08	-0.09	-0.03	-0.03	**0.80**	**0.91**	**0.56**	**0.90**	**0.89**	0.47	-0.41	-0.34	**-0.52**	0.07	0.13	-0.32	-0.27	0.23	-0.31	-0.44	-0.37	0.37	0.15	0.15	0.11	-0.45	1	0.01	0.22
Ta	**0.64**	-0.40	-0.08	-0.26	-0.24	-0.22	-0.12	0.05	0.48	-0.44	-0.43	**-0.53**	-0.39	-0.36	**-0.54**	0.47	0.40	**0.61**	**0.65**	-0.38	0.29	0.01	-0.31	0.06	0.20	0.23	0.06	0.15	0.15	**0.75**	**0.61**	-0.39	1	0.25
Pb	-0.04	0.24	0.14	0.02	-0.16	-0.10	-0.16	-0.08	-0.11	0.16	0.18	0.12	0.19	0.21	0.04	-0.20	-0.30	0.13	0.23	-0.27	-0.19	-0.21	0.00	-0.22	0.00	0.43	0.18	0.35	0.35	-0.03	0.13	0.15	-0.04	1

Preprints.org (www.preprints.org) | NOT PEER-REVIEWED | Posted: 11 October 2024 doi:10.20944/preprints202410.0793.v1

4. Results

4.1. Minerals in the Clay Fraction of Sediments

Kaolinite is the most dominant mineral, followed by minor illite, gibbsite and traces of goethite and quartz in the clay fraction of sediments from Kerala, Karnataka and Goa (Figure 2). The clay minerals on the continental shelf sediments off Goa, Karnataka and Kerala also showed abundant kaolinite followed by illite, gibbsite and goethite, with decreasing proportions of gibbsite as one moves from Kerala to Goa (Rao and Rao, 1995; Kessarkar et al., 2003). The clay minerals in the river sediments from Maharashtra and Gujarat showed predominant smectite, followed by kaolinite and chlorite and minor illite and quartz and, traces of feldspar (Figure 2). Very high proportions of smectite with minor kaolinite and illite were reported in the sediments from Narmada and Tapti Rivers (Naidu et al., 1985) and on the continental shelf off the Deccan Traps (Rao and Rao, 1995; Kessarkar et al., 2003).

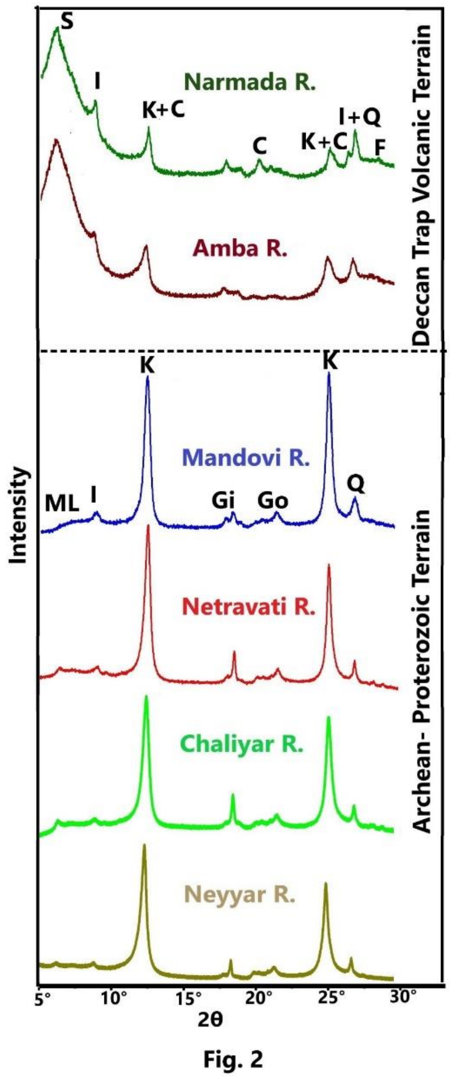

Figure 2. Selected X-ray diffractograms of the clay fraction of sediments. S—smectite, K—kaolinite, I—illite, C—chlorite, Gi—gibbsite, Go—goethite, Q—quartz and F—feldspar.

4.2. Distribution of Major Elements

Figure 3 shows the Post Archean average Australian Shale (PAAS) -normalized distribution of major element oxides in river sediments from each state. In general, the sediments are depleted with SiO_2, MgO, CaO, Na_2O and K_2O and enriched with Al_2O_3, Fe_2O_3, MnO, TiO_2 and P_2O_5 relative to PAAS

Preprints.org (www.preprints.org) | NOT PEER-REVIEWED | Posted: 11 October 2024 doi:10.20944/preprints202410.0793.v1

in both fractions. However, the relative enrichment / depletion of these oxides varies differently in river sediments of different states and terrains. The sediments weathered from the Archean-Proterozoic terrain (A-P terrain) are more enriched with Al_2O_3, Fe_2O_3 and P_2O_5, while those weathered from the Deccan Trap terrain (DT terrain) are enriched with MgO, CaO and TiO_2 in both fractions (Table 1). The mean Al_2O_3 content gradually decreased for the sediments from Kerala (23.5%) to Gujarat (14.43%). The mean Fe_2O_3 content, however, increased for the clays from Kerala (11.8%) to Goa (13.2%), but low mean values are characteristic for Maharashtra (10.75%) and Gujarat (8.9%). The mean SiO_2/Al_2O_3 ratio increased gradually from Kerala (1.45) to Gujarat (3.29) in the clay fraction of sediments (Table 1). Indeed, the mean ratio is much lower for the clays of Kerala (1.45), Karnataka (2.22) and Goa (2.24) than the Upper Continental Crust (UCC: 4.33) and PAAS (3.32). The mean ratio for the clay fraction of sediments was 2.64 for Maharashtra and 3.29 for Gujarat. The mean SiO_2/Al_2O_3 ratio was 2.99±0.61 for the silt fraction of sediments from A-P terrain and 3.43±0.66 for DT terrain (Table 1). The mean Fe_2O_3/Al_2O_3 ratios gradually increased in the clay fraction of sediments from Kerala (0.5) to Karnataka (0.64) and then to Goa (0.74) of the A-P terrain, but remained at 0.64 in DT terrain. The mean ratios, however, were much higher than in UCC (0.36) and PAAS (0.38). Similarly, the mean Fe_2O_3/Al_2O_3 ratio for the silt fraction of sediments was higher for the A-P terrain (0.54) than DT terrain (0.22). The Al_2O_3/TiO_2 ratio of the sediments gradually decreased from Kerala in the south to Gujarat in the north. For example, the mean ratio decreased from 21.22 to 13.71 for the clay and from 18.3 to 11.5 for silt fractions of sediments from the A-P terrain. Similarly, the mean ratio decreased from 11.98 to 10.39 for the clay and from 6.37 to 6.12 for silt fractions of sediments from the DT terrain. The Al_2O_3/TiO_2 ratios for UCC and PAAS are 24.29 and 18.9, respectively (Table 1).

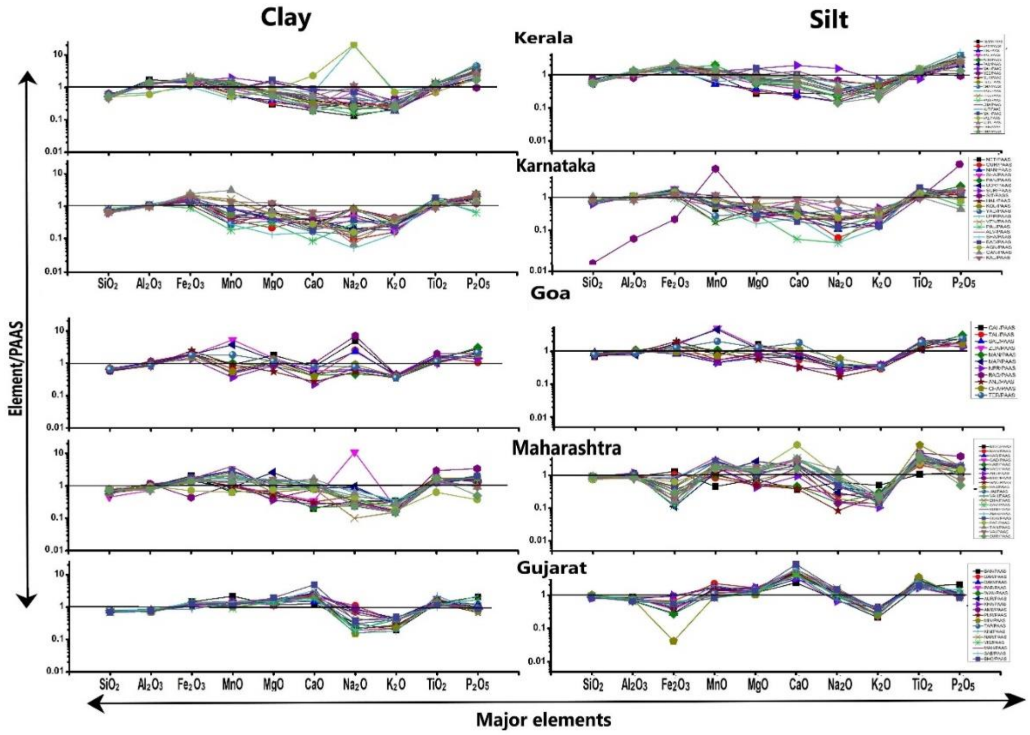

Fig. 3

Figure 3. Post Archean average Australian Shale (PAAS) – normalized distribution of major element oxides in the clay and silt fractions of sediments in the rivers from each state.

4.3. Weathering Indices

To better understand the degree of chemical weathering and extent of lateritisation, weathering indices such as chemical index of alteration (CIA), plagioclase index of alteration (PIA), index of chemical variability (ICV), mafic index of alteration (MIA) and intensity of lateritisation (IOL) are determined, using the oxides of major elements.

Preprints.org (www.preprints.org) | NOT PEER-REVIEWED | Posted: 11 October 2024 doi:10.20944/preprints202410.0793.v1

The chemical index of alteration (CIA) is determined by the equation of Nesbitt and Young (1982).

$$CIA = [Al_2O_3 / (Al_2O_3 + CaO^* + Na_2O + K_2O)] \times 100$$

CIA values varied widely in both fractions of sediments. It ranged from 27 to 97 for the clay fractions and, from 47 to 96 for silt fractions of sediments (Table 1). Low CIA values in both fractions correspond to the sediments of Gujarat. The mean CIA values for the clay and silt fractions are 86 and 88 for sediments from the A-P terrain and, 80 and 72 for DT terrain, respectively. Figure 4A shows the plot of CIA values graphically in the A-CN-K diagram. The clay fractions of sediments from Kerala, Karnataka and Maharashtra plot close to Al_2O_3 pole indicating strong (intense) chemical weathering, while those from Goa and Gujarat plot in the intermediate to strong weathering region (Figure 4A). On the other hand, the silt fractions of sediments from Kerala and Karnataka exhibit strong weathering, while that of Goa and Maharashtra exhibit intermediate to strong weathering and, those from Gujarat exhibit weak to intermediate weathering (Figure 4A).

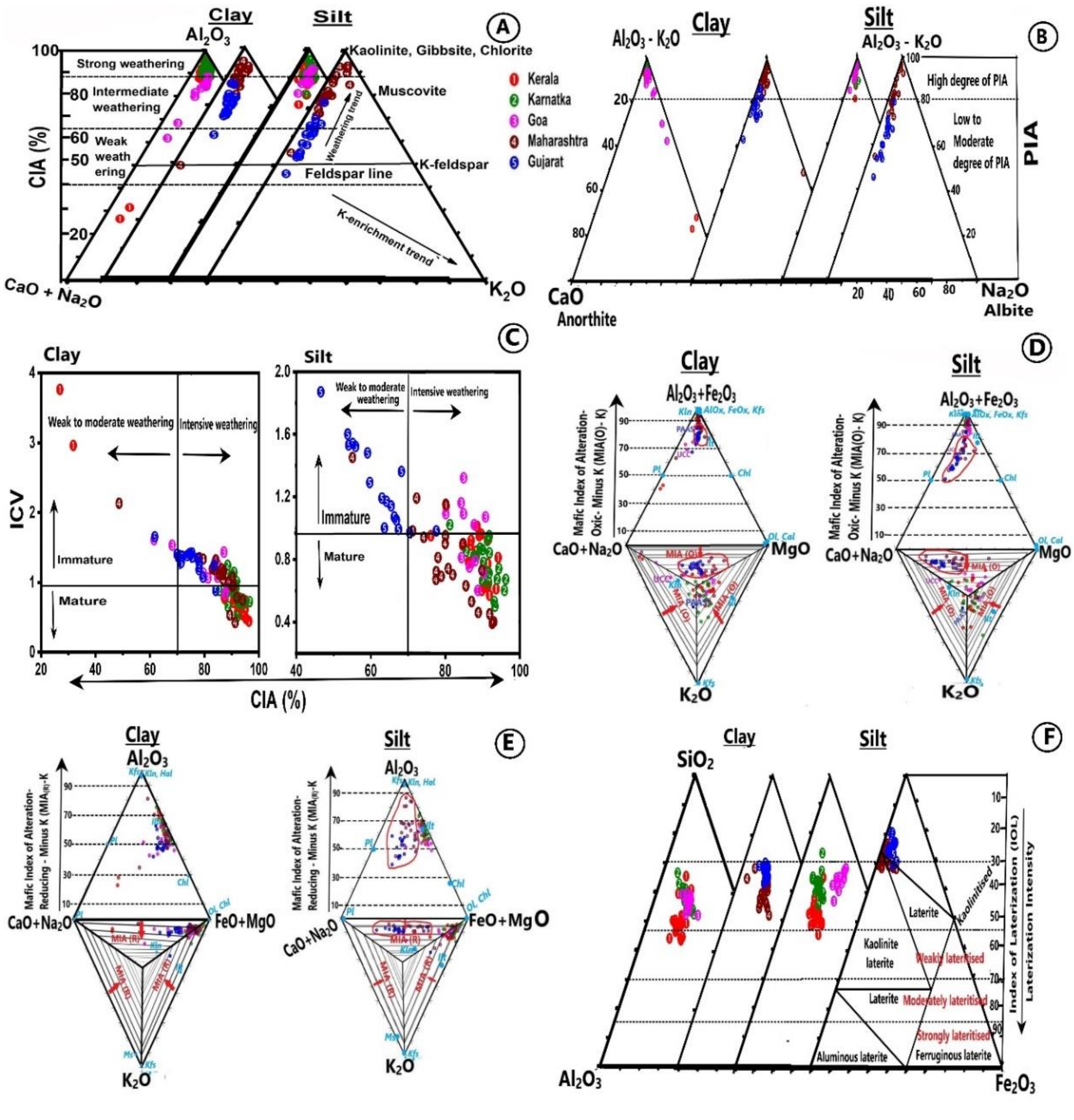

Fig. 4

Figure 4. Ternary diagrams showing (A) the plots of Al_2O_3–(CaO+Na_2O)–K_2O along with chemical index of alteration (CIA) (after Nesbitt and Young, 1982) and (B) (Al_2O_3– K_2O)-CaO-Na_2O along with plagioclase index of alteration (PIA) (after Fedo et al., 1995, 1996). (C) Plot of chemical index of alteration (CIA) vs index of chemical variability (ICV) (after Cox et al., 1995), (D) Tetrahedral plot of

Preprints.org (www.preprints.org) | NOT PEER-REVIEWED | Posted: 11 October 2024 doi:10.20944/preprints202410.0793.v1

AF–CN–K–M ((Al_2O_3+Fe_2O_3)–(CaO+Na_2O)–(K_2O)–(MgO)) (modified after Babechuk and Fedo, 2022), (E) Tetrahedral plot of A–CN–K–FM ((Al_2O_3)–(CaO+Na_2O)–(K_2O)–(FeO+MgO)) (modified after Babechuk and Fedo, 2022). (F) Ternary plot of S–A–F (SiO_2– Al_2O_3–Fe_2O_3) showing the degree of lateritisation and Index of lateritisation (IOL) (modified after Schellmann, 1986; Babechuk et al., 2014).

The plagioclase index of alteration (PIA) is widely used to quantify the degree of weathering of plagioclase feldspar. It is determined by the equation of Fedo et al. (1995, 1996).

$$PIA = (Al_2O_3 - K_2O) / (Al_2O_3 + CaO^* + Na_2O - K_2O) \times 100$$

where all elements are in molecular proportions.

Fedo et al. (1995, 1996) reported that the sediments subjected to strong chemical weathering exhibit a PIA value of 100 and, PIA value of 50 represents unweathered plagioclase. In this study, the PIA values are in the range 21 to 94 for the clay fractions and 41 to 94 for the silt fractions of sediments (Table 1). The average PIA values for the clay fractions of sediments from A-P terrain and DT terrain are 86 and 80, respectively. Similarly, the average PIA values for the silt fraction of sediments from the A-P terrain and DT terrain are 88 and 71, respectively. The plot of major element oxides in the ternary diagram ((Al_2O_3– K_2O)-CaO–Na_2O) indicates that the sediments from Kerala, Karnataka, Goa and Maharashtra exhibit high degree of plagioclase weathering, while those from Gujarat exhibit low to moderate degree of plagioclase weathering (Figure 4B).

The **index of chemical variability (ICV)** is used as a proxy indicator to assess the role of mineralogical maturity of the sediments. It is determined by the equation of Cox et al. (1995).

$$ICV = (Fe_2O_3 + K_2O + Na_2O + CaO + MgO + MnO + TiO_2)/Al_2O_3.$$

Typical rock forming minerals such as feldspars, amphiboles, and pyroxenes have ICV value >1, whereas the alteration products like kaolinite, illite, and muscovite have ICV value < 1 (Cox et al., 1995; Cullers, 2000). High ICV values imply compositionally immature sediments due to high content of non-clay silicate minerals, whereas low ICV values correspond to mature sediments deposited in areas of sediment recycling and intense chemical weathering. The ICV values varied widely in both fractions of sediments (Table 1). The mean ICV values of the clays from Kerala, Karnataka and Goa are 0.97, 0.87 and 1.21, respectively, with an overall mean of 1.02 for the A-P terrain. The mean ICV values of the clays from Maharashtra and Gujarat are 1.08 and 1.31, respectively, with an overall mean of 1.20 for the DT terrain. Similarly, the mean ICV values are <1 for the silts from Kerala, Karnataka, Goa and Maharashtra and, 1.28 (range: 0.97–1.87) for Gujarat. The plot of ICV vs. CIA (Figure 4C) indicates that the clays from Kerala, Karnataka and Maharashtra are intensely weathered and compositionally mature, whereas the clays from Goa and Gujarat are intensely weathered, with a few showing compositional immaturity (Figure 4C). On the other hand, most of the silt fractions of sediments from Kerala, Karnataka and Maharashtra are intensely weathered and mature. A few silt samples from Goa are immature but intensely weathered. Almost all silt samples from Gujarat are compositionally immature and weakly weathered (Figure 4C).

Babechuk et al. (2014) proposed **Mafic Index of Alteration (MIA)** to quantify the total loss of mobile elements relative to that of immobile elements. Subsequently, Babechuk and Fedo (2022) proposed $MIA_{(O)}$ and $MIA_{(R)}$, respectively for oxidative and reductive weathering, to separate the effects of feldspars (both plagioclase and K-feldspar) and mafic mineral weathering and, addition of labile elements during diagenesis / metasomatism. Following Babechuk and Fedo (2022),

$$MIA_{(O)} = [(Al_2O_3 + Fe_2O_{3(T)}) / (Al_2O_3 + Fe_2O_{3(T)} + MgO + CaO + Na_2O + K_2O)] \times 100$$

$$MIA_{(R)} = [(Al_2O_3) / (Al_2O_3 + FeO_{(T)} + MgO + CaO + Na_2O + K_2O)] \times 100$$

Table 1 shows the values for $MIA_{(O)}$ and $MIA_{(R)}$. In general, the $MIA_{(O)}$ values are close to that of CIA. The mean $MIA_{(O)}$ values range from 82 to 91 for the clay and from 84 to 91 for silt fractions of sediments from the A-P terrain. It ranges from 74 to 84 for the clay and 62 to 75 for silt fractions of

Preprints.org (www.preprints.org) | NOT PEER-REVIEWED | Posted: 11 October 2024 doi:10.20944/preprints202410.0793.v1

sediments from the DT terrain, with low values in both fractions corresponding to Gujarat. The $MIA_{(R)}$ values are much lower than $MIA_{(O)}$ in both size fractions. The mean $MIA_{(R)}$ values are 55 and 50 for the clay fractions and 50 and 57 for the silt fractions of sediments from A-P terrain and DT terrain, respectively.

Babechuk and Fedo (2022) used tetrahedral plots to better understand the processes preserved at different stages of weathering both in modern and ancient weathering profiles. They proposed AF-CN-K-M tetrahedral plot (Figure 4D), useful for oxidative weathering, where Fe is retained alongside Al across all stages of incipient to advanced weathering. One ternary diagram (AF-CN-M) of the AF-CN-K-M tetrahedron is integrated with $MIA_{(o)}$–K weathering index (Figure 4D). The sediments from A-P terrain and Maharashtra of the DT terrain showed MIA(o) values >80 in both size fractions and plot very close to AF pole in AF-CN-M diagram indicating extreme leaching and net loss of Ca, Na, K and Mg, released from plagioclase and mafic minerals and Fe is retained via oxyhydroxide development (Babechuk and Fedo 2022). This agrees with the results from X-ray diffraction studies, where Al is retained as gibbsite and Fe as goethite (Figure 2) in the sediments from A-P terrain. The sediments from Gujarat plot slightly away from AF pole (with MIA(o) values 50 to 80 in both fractions) suggesting intermediate leaching of labile elements. However, in another ternary diagram (CN-K-M) of the tetrahedron, our samples plot in the central inner space designated for $MIA_{(o)}$ (Figure 4D), indicating strong leaching of labile elements and, subsequent diagenesis has not obscured the chemical weathering effects.

Babechuk and Fedo (2022) also proposed A-CN-K-FM tetrahedral plot (Figure 4E), useful to study reductive weathering, where Fe is lost and/or redistributed in the system. One ternary diagram (A-CN-FM) of the tetrahedron is integrated with $MIA_{(R)}$-K weathering index (Figure 4E). Our samples plot slightly away from FM pole and slightly towards A pole in the A-CN-FM diagram, suggesting advanced weathering stage where Fe+Mg were lost. Since our sediment samples show high values of Fe and, some Fe may have retained as goethite. The average $MIA_{(R)}$ values for clay (55±7.1) and silt (59±4.9) fractions from A-P terrain may indicate only loss of Mg during advanced weathering of sediments. In another ternary diagram (CN-K-FM) of the tetrahedron (Figure 4E), our samples plot close to FM pole, but not in the inner space designated for $MIA_{(R)}$ reduction, implying subsequent diagenesis has not obscured the chemical weathering effects. The silt samples from Gujarat plot mid-way between AN and FM (Figure 4E) suggesting intermediate weathering has minimal effect on labile elements.

Babechuk et al. (2014) also proposed the equation to quantify the **index of lateritisation** (IOL) as

$$IOL = [(Al_2O_3 + Fe_2O_3) / (SiO_2 + Al_2O_3 + Fe_2O_3)] \times 100$$

The mean IOL values for the clay and silt fractions of sediments are in the range from 45 to 40 for A-P terrain and, 35 to 26 for DT terrain (Table 1). Babechuk et al. (2014) reported IOL values <40 for unweathered mafic rocks and an IOL value of 35.7 for unweathered Deccan Trap Basalts. Following these authors, the samples from A-P terrain fall in the category of weakly lateritised, and those from DT terrain are non-lateritised. This agrees well with the mineralogy of the clay fraction contains, kaolinite, gibbsite and goethite indicating lateritised sediments from A-P terrain (Figure 2). Schellmann (1986) proposed triangular plot of SiO_2 (S)- Al_2O_3 (A)- Fe_2O_3 (F) (S-A-F diagram) to identify whether the weathering residues are kaolinitised, lateritised or bauxitised. The clay fractions of all sediments plot in the region ‘weakly lateritized’ to ‘kaolinitised’, with samples from Kerala exhibiting weakly lateritised to samples from Gujarat kaolinitised. The silt fractions of sediments from Maharashtra and Gujarat are neither kaolinitised nor lateritized on S-A-F diagram (Figure 4F).

4.4. Distribution of Trace Elements

The PAAS-normalized distribution of trace elements in the sediments from different states (Figure 5) showed strong depletion of alkaline earth elements (Rb, Sr, Cs, Ba). The Th, U, La and Ce are enriched relative to PAAS in the sediments of Kerala and Karnataka, but depleted as one moves towards Goa, Maharashtra and Gujarat. The transition trace elements (TTE: Sc, V, Cr, Co, Ni) are enriched relative to that of PAAS in the sediments of all rivers (Figure 5). The TTE content of the

Preprints.org (www.preprints.org) | NOT PEER-REVIEWED | Posted: 11 October 2024 doi:10.20944/preprints202410.0793.v1

sediments is higher in the silt fractions than in clay fractions. Moreover, the ΣTTE is higher in the sediments from DT terrain than in A-P terrain (Tables 2 and 3). The distribution of Cu and Zn is same as that of TTE. The Ga content is enriched relative to that of PAAS, with higher values in the sediments from A-P terrain than in DT terrain (Tables 2 and 3). Among the high-field strength elements (HFSE: Zr, Hf, Ta, Nb and Y), Nb is depleted relative to PAAS in the sediments of all rivers. In the clay fraction of sediments, the mean values of Zr, Hf, Ta and Y are lower for A-P terrain than DT terrain (Table 2). Moreover, the mean values of these elements from different states are close to that of UCC in the A-P terrain. In the silt fractions, the mean values of Zr, Hf and Ta are much higher and Y much lower for the sediments from A-P terrain than DT terrain (Figure 5A).

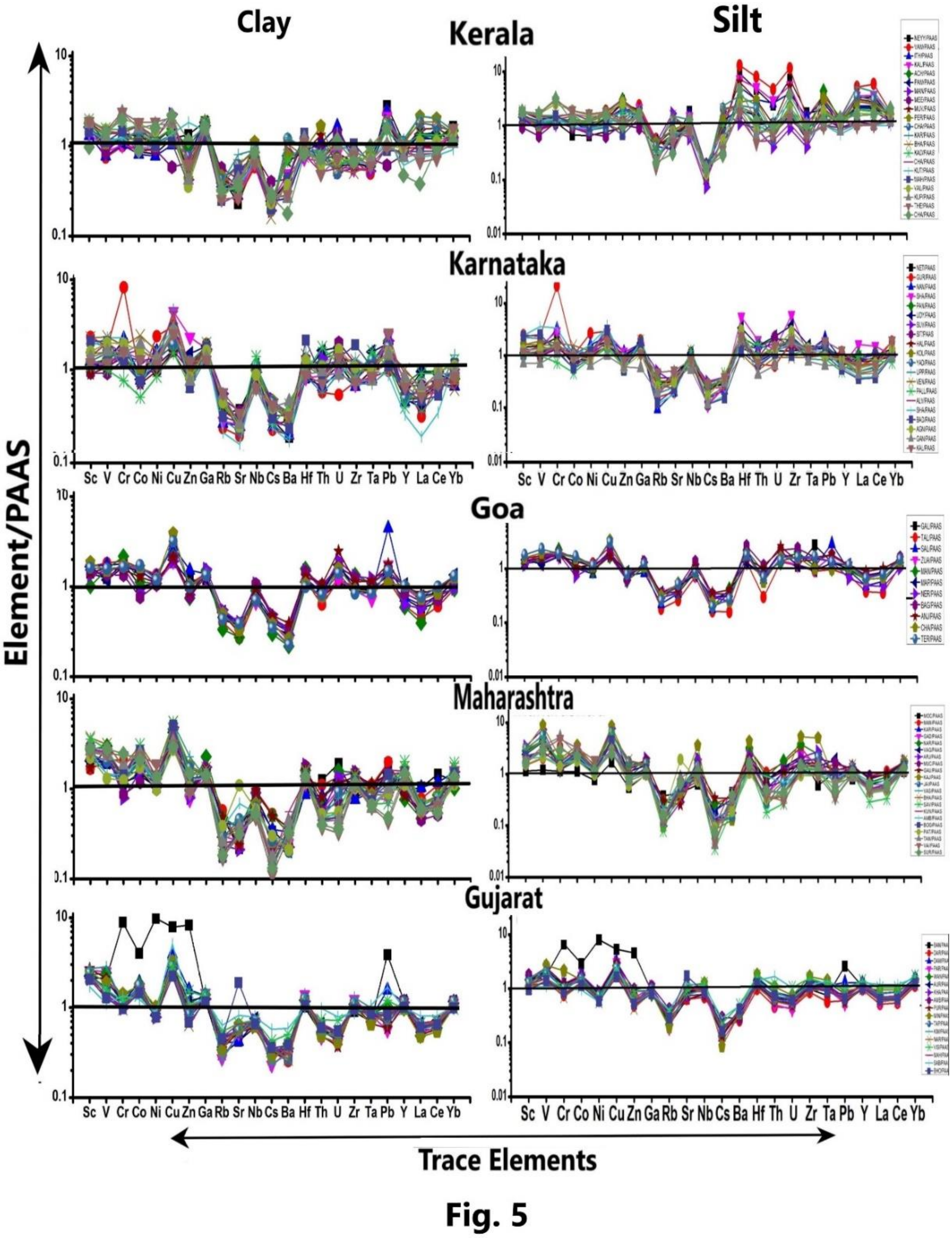

Figure 5. Post Archean average Australian Shale (PAAS) – normalized distribution of trace elements in the clay and silt fractions of sediments in the rivers from each state.

Preprints.org (www.preprints.org) | NOT PEER-REVIEWED | Posted: 11 October 2024 doi:10.20944/preprints202410.0793.v1

Total Trace elements (ΣTE) content: A total of 23 trace elements, excluding rare earth elements (REE), are considered in this study. Figure 6A shows the distribution of total-trace elements content (ΣTE) for the clay and silt fractions of sediments, separately. Sai Babu et al. (2024) reported REE distribution of these sediments. The distribution of trace elements along with a few REE (La, Ce, Yb, Y) are given in Tables 2 and 3 and considered here for discussion. The ΣTE varied from 991.6 to 2027.1 µg/g in the clay fractions and, from 1081.1 to 3848.6 µg/g in silt fractions of sediments from different states. The mean ΣTE of the sediments was much lower in the clay fraction than their silt fractions in all states (Figure 6a). Within the clay fractions, the ΣTE of Maharashtra was high compared to other states (Table 2). The mean ΣTE of the clay fraction of sediments from all rivers (1473.05 µg/g) was lower than their silt fraction (1878.62 µg/g), UCC (1650.57 µg/g; Rudnick and Gao, 2003) and PAAS (1807.09 µg/g; Pourmand et al., 2012). The silt fractions of sediments showed broad peaks of high ΣTE corresponding to the rivers of Kerala and Maharashtra, and sharp peaks of high ΣTE for the sediments at the border rivers of Kerala - Karnataka and, Maharashtra -Gujarat (Figure 6a). The peaks of high ΣTE correspond to broad peaks of high ΣREE in the sediments of Kerala (Figure 6b), but in other states ΣREE distribution is significantly different from that of ΣTE (Figure 6a and b)

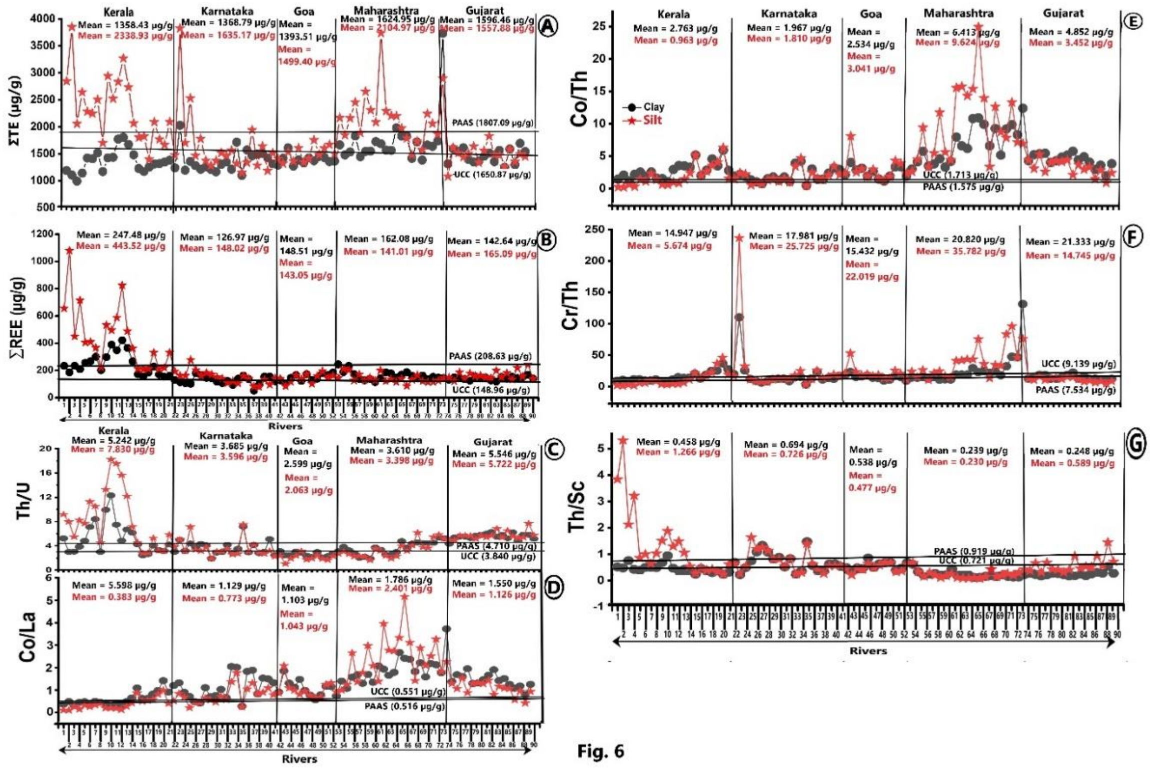

Figure 6. (A) The total trace element content (∑TE) and (B) total rare earth element content (∑REE), (C) Th/U, (D) Co/La, (E) Cr/Th, (F) Co/Th and (G) Th/Sc ratios in the clay and silt fractions of sediments in the rivers along the west coast of India.

Trace element ratios: Figure 7A shows the distribution of Th/U ratio in the sediments of all rivers. The Th/U ratio of the clays are lower than in silts. The mean Th/U ratios for the clay and silt fractions of sediments from A-P terrain (4.08 and 5, 22, respectively) and DT terrain (4.47 and 4.44) are higher than in UCC (3.84; Tables 2 and 3). The average Th/U ratios for the clay (5.2) and silt (7.8) fractions of sediments from Kerala are much higher than in UCC and PAAS (4.71; Tables 2 and 3) and, peak high Th/U ratio broadly coincides with peak ΣTE (Figure 6c). The mean Th/U ratios for the clay and silt fractions of sediments from Karnataka (3.68 and 3.56, respectively) and Maharashtra (3.6 and 3.4) are close to that of UCC, but much lower for Goa (2.6 and 2.06) and higher for Gujarat (5.5 and 5.72) than UCC and PAAS (Tables 2 and 3). The Th content and Th/U ratio of the sediments were plotted on the binary diagram of Gu et al. (2002). It showed significant positive correlation between the two in the sediments from A-P terrain and, weak correlation in clay fractions and, moderate positive correlation in the silt fraction of sediments from DT terrain (Figure 7B).

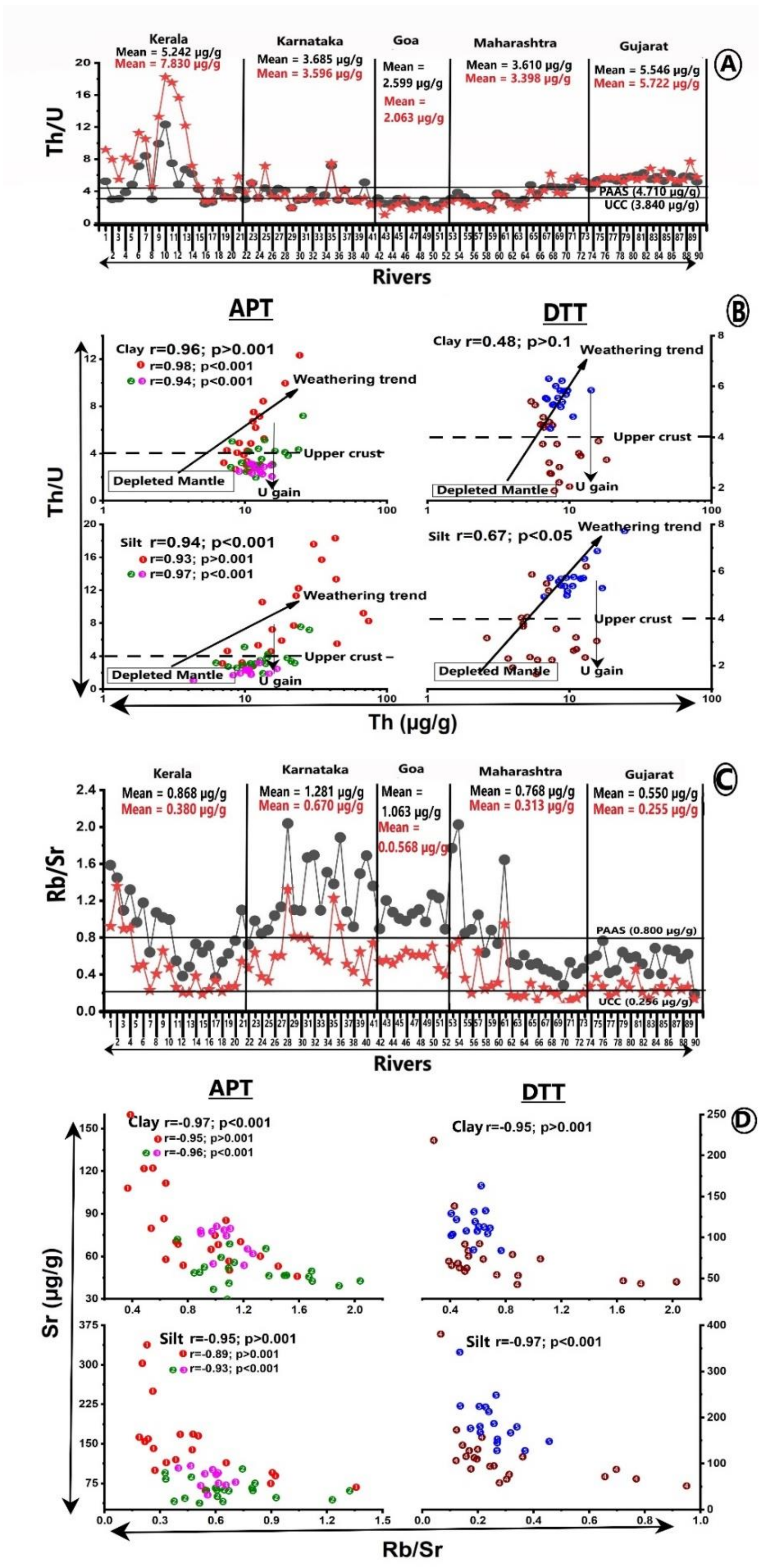

Fig. 7

 doi:10.20944/preprints202410.0793.v1

Figure 7. (A) Variations in the Th/U ratio, (B) binary plot of Th content versus Th/U ratio (Fields and trends from Gu et al. 2002), (C) Variations in the Rb/Sr ratio and (D) binary plot of Rb/Sr versus Sr content (Xu et al., 2010) in the clay and silt fractions of sediments in the rivers of western India.

Figure 7C shows the distribution of Rb/Sr ratio in the sediments of all rivers. Unlike Th/U ratio, the Rb/Sr ratios are much higher in the clay fractions than their silt fractions, but both fractions showed similar trend in their distribution. The mean Rb/Sr ratios for the clay fractions of sediments from A-P terrain (1.07) and DT terrain (0.67) were much higher than in UCC (0.26; Table 2). The mean Rb/Sr ratios for the clay and silt fractions of sediments from Kerala (0.87 and 0.38, respectively), Karnataka (1.28 and 0.67), Goa (1.06 and 0.56), Maharashtra (0.77 and 0.31) and Gujarat (0.55 and 0.25) showed lower mean ratios for the silt fractions from DT terrain (Maharashtra and Gujarat) and these ratios were close to that of UCC. The binary plot of Rb/Sr ratio against Sr content of the sediments (Xu et al., 2010) shows strong negative correlation between the two in both fractions of sediments and from both terrains (Figure 7D).

4.5. Relationships of Major and Trace Elements

Table 4 is the correlation matrix of elements for the clay fraction of sediments, separately for A-P terrain and DT terrain. Figure 8 shows the important binary plots between the elements. Within the A-P terrain, Al_2O_3 showed negative correlation with CaO, Na_2O, MgO and K_2O (Figure 8a) and no correlation with other major elements (Table 4). The TiO_2 showed strong correlation with Zr, Hf and Nb (Figure 8b), while P_2O_5 showed strong correlation with Sr, Ba and ∑REE (Figure 8c). Moderate to strong correlation exists among U, Th, Nb, Cs and Ta. The Fe_2O_3 and MnO showed strong correlation with V and Co (Figure 8d). On the other hand, the sediments from DT terrain, however, showed negative correlation of Al_2O_3 with CaO, MgO and Na2O and strong correlation with P_2O_5 (Figure 8e). The Al_2O_3 also showed moderate to strong correlation with Zr, Hf, U, Ga Nb and Ta. The Fe_2O_3 showed positive correlation with ∑REE (Figure 8f), U and Co. TiO_2 showed strong correlation with Zr, Hf, V and Ga. Strong correlation exists among TTE (Sc, Co, Cr, Ni, Cu and Zn; Figure 8g) elements and TTE with Zr and Hf (Figure 8h).

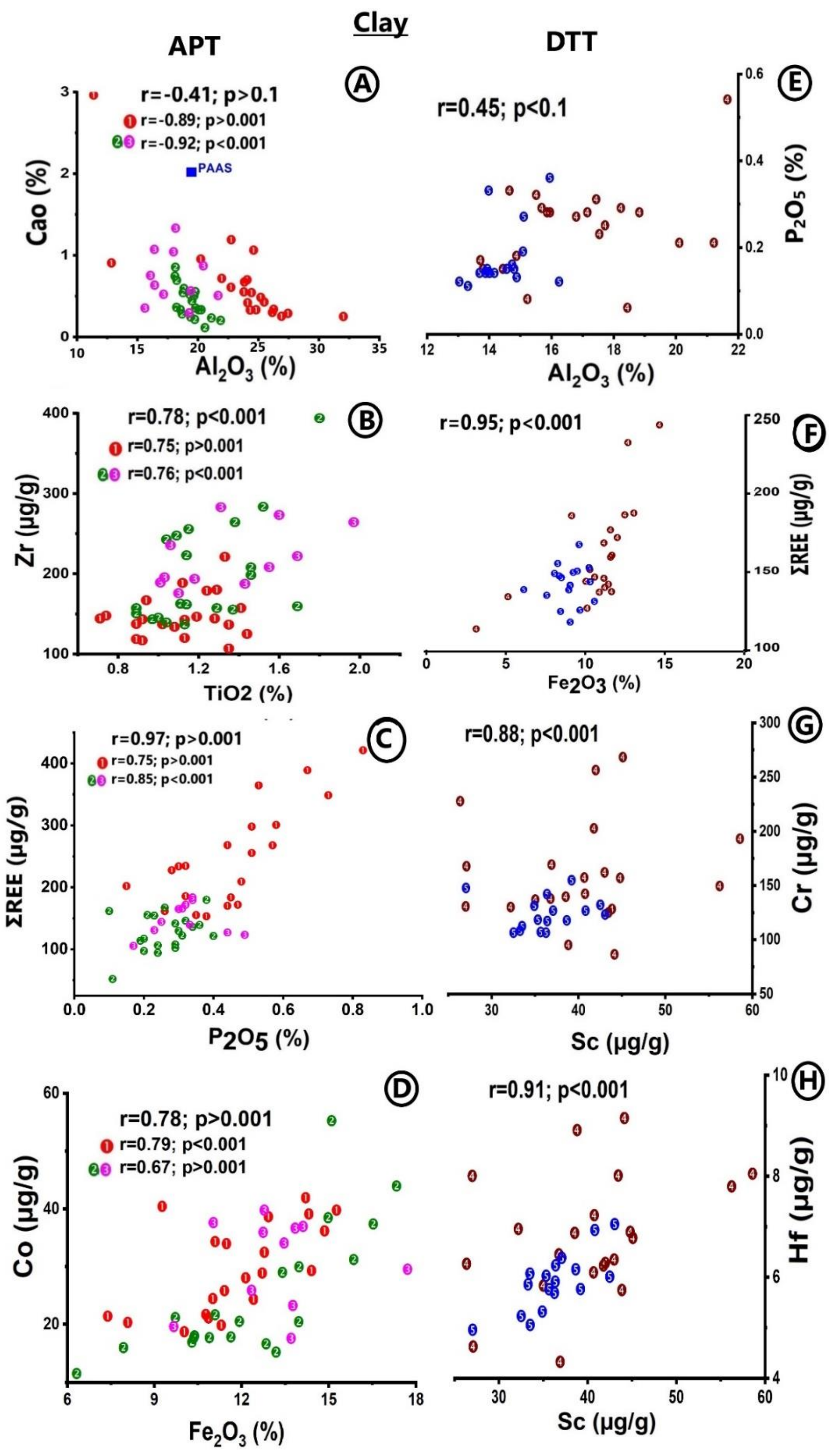

Fig. 8

Figure 8. Selective correlation plots in the clay fraction of sediments: Correlation (A) between Al_2O_3 and CaO, (B) TiO_2 and Zr, (C) P_2O_5 and ∑REE and (D) Fe_2O_3 and Co from the sediment of A-P terrain. Correlation (E) between Al_2O_3 and P_2O_5, (F) Fe_2O_3 and ∑REE, (G) Sc and Cr and (H) Sc vs Hf from the sediments of DT terrain.

Preprints.org (www.preprints.org) | NOT PEER-REVIEWED | Posted: 11 October 2024 doi:10.20944/preprints202410.0793.v1

5. Discussion

5.1. Mineralogy and Major Element Geochemistry—Stages of Weathering

The Western Ghats (WG) comprise of Archean-Proterozoic formations (A-P terrain) in Kerala, Karnataka and Goa and, continental flood (Deccan Trap) basalts (DT terrain) in Maharashtra and Gujarat, being weathered under humid tropical climatic conditions. Since the rivers are draining the WG, they obviously carry the weathering products of rocks subjected to chemical weathering, prevalent under tropical conditions. Kaolinite is a product of intense chemical weathering (Chamley, 1989). Occurrence of abundant kaolinite along with gibbsite in the sediments from A-P terrain (Figure 2) indicates that the hinterland rocks were subjected to intense chemical weathering and lateritisation and/or, the sediments are weathered from laterites. Babechuk and Fedo (2022) reported that the breaking down of 2:1 clays and formation of dominant 1:1 clay such as kaolinite, and Al- and Fe -(oxy)-(hydr)oxides such as gibbsite and goethite indicate that the sediments have undergone intense to extreme weathering conditions. Therefore, the clay minerals from A-P terrain (Figure 2) represent extreme chemical weathering and their derivation from laterites (see below). The increase in gibbsite content in the offshore sediments from Goa to Kerala was attributed to increase in lateritisation from Goa to Kerala (Rao and Rao, 1995).

Smectite is the dominant weathering product of Deccan Trap basalts under tropical conditions. Abundant smectite together with minor kaolinite, chlorite and illite in the sediments of Maharashtra and Gujarat (Figure 2) thus reflect dominant weathering products from basalts. The sediments with abundant smectite and minor kaolinite and chlorite indicate the abundant occurrence of 2:1 clay (smectite) and early stage of 1:1 clay (kaolinite) formation, suggesting advanced to intense stage of chemical weathering, according to the classification of Babechuk and Fedo (2020).

The depletion of labile elements such as Ca, Mg, Na and K relative to PAAS (Figure 3) indicates that they are leached and carried away as a solute during chemical weathering of source rocks. The extent of leaching of labile elements is much higher in the sediments from A-P terrain than in DT terrain. Weathering indices, such as CIA and PIA indeed point out that the clay fractions of sediments from Kerala, Karnataka and Maharashtra exhibit strong weathering or, high degree of plagioclase weathering (Figure 4), while those from Goa and Gujarat exhibit strong to intermediate weathering. A few silt samples from Kerala, Karnataka, Goa and Maharashtra exhibit intermediate weathering and all silts from Gujarat exhibit weak to intermediate weathering (Figure 4A and B). The $MIA_{(O)}$ values are close to that of CIA (Table 1) and point out extreme leaching and net loss of Ca, Na, K and Mg, released probably from plagioclase and mafic minerals. The $MIA_{(R)}$ values indicate only loss of Mg during advanced weathering of sediments and, chemical weathering effects are not obscured by subsequent diagenesis. The intensity of laterization simply point out kaolinite laterite for the sediments of Kerala and kaolinization in all other sediments (Figure 4F). In other words, lateritisation decreased from Kerala to Gujarat and sediments of Maharashtra and Gujarat exhibit no lateritisation and weathered due to advance chemical weathering.

5.2. Major Element Chemistry—Provenance

Major element data provide evidence regarding sedimentary provenance and effects of sedimentary processes such as weathering and sorting. The SiO_2/Al_2O_3 ratio is close to that of UCC or higher for the sediment weathered from intense chemical weathering of source rocks and, much lower than in UCC for the sediment weathered from laterites. This ratio is <1.33 for laterites, 1.33–2.0 for lateritic soils and >2.0 for non-lateritic, chemically weathered tropical soils (Martin and Doyne, 1927; Narayanaswamy, 1992). The SiO_2/Al_2O_3 ratio, however, can range from 1.33 to 2.2 in lateritic soils (Martin and Doyne, 1927). The mean SiO_2/Al_2O_3 ratio for the clay fractions of sediments from Kerala (1.45), Karnataka (2.22) and Goa (2.24) and, silt fraction of sediments from Kerala (1.71) suggests that they resemble lateritic soils. The mean SiO_2/Al_2O_3 ratio for the silts from Karnataka (2.6) and Goa (2.81) suggests dilution of lateritic soils by material weathered from the hinterland. The gradually decreasing Al_2O_3 content coinciding with increasing Fe_2O_3 content in the clay fraction of sediments from Kerala to Goa (Table 1) and, increasing mean Fe_2O_3/Al_2O_3 ratio from 0.5 in Kerala to

0.64 in Karnataka and then to 0.74 in Goa suggest increase in particulate iron, probably from Fe-Mn ore mines, located in north Karnataka and Goa (Gokul et al., 1985; Dhoundial et al., 1987; Naqvi, 2005; Desai et al., 2009). As rivers from northern Karnataka and Goa drain these open cast mines and weathered material from the ores together with lateritic material are transported as suspended and bed load and deposited in the lower reaches of rivers and estuaries. Several workers reported ore material -dominated sediments in the rivers and estuaries of northern Karnataka and Goa (Shynu et al., 2011, 2014; Prajith et al., 2015; Kessarkar et al., 2015; Suja et al., 2017). Therefore, the sediments of Karnataka and Goa are lateritic soils admixed with ore material. Sai Babu et al. (2024) reported MREE- and HREE-enriched REE patterns with positive Ce and Eu anomaly in the clay and silt fractions of sediments from the rivers of northern Karnataka and Goa and suggested that these sediments consist of weathered material from source rocks, Fe-Mn ores and laterites. On the other hand, the mean SiO_2/Al_2O_3 ratios of the clay and silt fractions of sediments from Maharashtra (2.54 and 2.99, respectively) and Gujarat (3.29 and 3.97) suggest that the sediments are non-lateritic and chemically weathered soils. However, these sediments contain high Fe_2O_3 (mean: 9.93%) and TiO_2 (mean: 1.48%) in the clay fractions. Moreover, the much lower mean Al_2O_3/TiO_2 ratios for the clay (11.7) and silt (6.2) fractions of sediments from DT terrain than in UCC (24.29) point to Ti-enrichment. Furthermore, strong correlation of TiO_2 with Zr, Hf, Nb, V and Ga (Figure 7; Table 4) suggests Ti association with heavy metal-enriched minerals, i.e., heavy minerals such as rutile and ilmenite. In other words, the sediments from DT terrain contain Fe- and Ti-enriched minerals, magnetite and ilmenite and rutile, abundantly reported from the Deccan Trap basalts.

5.3. Relationships among Major Elements and Trace Elements

Strong correlation among labile alkali and alkaline earth elements and their negative correlation with Al_2O_3, Fe_2O_3 and TiO_2 in the sediments from both terrains (Table 4; Figure 8a)) may be related to chemical weathering of source rocks, wherein labile elements are transported as dissolved species, and immobile elements such as Al, Fe and Ti are enriched in solid detritus. The correlation of TiO_2 with Zr, Hf and Nb in the sediments from both terrains (Table 4; Figure 8b) implies association of these elements with heavy minerals. Strong correlation of Fe_2O_3 and MnO with Co (Figure 8d) suggest Co adsorbed onto Fe-Mn oxy-(hydr) oxides. The moderate to strong correlation of P_2O_5, Fe_2O_3 and MnO with ΣREE in the clay fractions of sediments from A-P terrain (Figure 4; Figure 8C) suggests REEs released during weathering are bound to secondary mineral phases such as Fe-Mn oxy-(hydr)oxides and phosphate. Strong positive correlation of ΣREE with Fe_2O_3 (Figure 8F) and moderate correlation with Al_2O_3 (Table 4) in the sediments from DT terrain suggests that the clay minerals and Fe-oxy-(hydr)oxides are important host for REE. It appears that that the primary host for REE are secondary weathering products such as Fe-ocy hydroxides and phosphate in the A-P terrain and, clay minerals and Fe oxy-(hydr)oxides in the DT terrain. Pourret et al. (2013) and Du et al. (2021) suggested that REE are adsorbed onto Fe-Mn oxy- (hydr) oxides and phosphates abundantly. The correlation of Sr and Ba with P_2O_5 in both terrains indicates that they are associated with secondary mineral phases like phosphates. Strong correlation of Al_2O_3 with Ga in both terrains (Table 4) suggests its association with clay minerals. High Ga content in the A-P terrain than DT terrain may be due to preferential binding of Ga with kaolinite and gibbsite-rich sediments. Several workers reported association of high Ga content with laterites (Narayanaswamy 1992; Abedini et al., 2014). Positive correlation of Al_2O_3 with Zr, Hf, U, Ga, Nb, Ta (Table 4) implies that these elements are immobile during weathering and associated with the weathered detritus. Within the DT terrain, strong correlation exists among TTE (Figure 8G) and, TTE (Sc, Co, Cr, Ni, Cu and Zn) are negatively correlated with Rb, Cs and Nb (Table 4) may be because TTE are retained and alkaline earth elements are removed during chemical weathering. High TTE and Yb contents and strong correlation of Yb with TTE (Table 4) suggest that TTE and heavy rare earth elements (HREE) like Yb occur in higher proportions in basalts. Sai Babu et al. (2024) reported PAAS-normalized MREE and HREE-enriched and LREE-depleted patterns in the weathered products of basalts. Correlation of REE with U, Th and Ta (Table 4) indicates that some REE are associated with heavy metal associated minerals (i.e., heavy minerals). Positive correlation of Zr and Hf with Sc, V and Ga and, positive correlation of U and Th

Preprints.org (www.preprints.org) | NOT PEER-REVIEWED | Posted: 11 October 2024 doi:10.20944/preprints202410.0793.v1

with Rb, Cs, Nb, Ta, Ga suggest a mixed source for these elements. It has been reported that the basalts are contaminated with crustal rocks away from Deccan Plateau and crustal rocks are exposed because of thin cover of Deccan basalts. Heavy monsoonal rains may have eroded these contaminated crustal rocks and released these metals to the sediments.

5.4. Factors Controlling ∑TE in the Sediments

Trace elements are usually associated with fine-grained sediments and heavy minerals. The low ∑TE or, ∑TE values close to that of UCC in the clay fractions and relatively high ∑TE in the silt fractions of sediments in rivers from different states (Figure 6A; Tables 2 and 3) imply that the trace elements released during chemical weathering are largely transported away from source rocks. As these rivers drain the Western Ghats (WG) mountain ranges, the steep slopes of the WG and, chemical weathering associated with heavy monsoonal rains (>250 mm/yr) in short duration (within 4 months during southwest monsoon—June to September) may have facilitated quick erosion of dissolved and particulate material from the weathering site and transportation into the rivers, resulting in low ∑TE in the clay fraction.

The peaks of high ∑TE in the silt fraction correspond to the sediments from Kerala and Maharashtra (Figure 6A). Moreover, the type of trace elements associated with ∑TE are different in both states. For example, the peak high ∑TE in the sediments of Kerala is associated with peaks of high Th/U and peak high ∑REE (Figure 6A-C), low Co/La, Cr/Th and Co/Th ratios (Figure 6D-F), peak high Th/Sc (Figure 6G) and higher HFSE elements relative to PAAS (Figure 5). It implies high ∑TE is associated with Th- and La-enriched minerals such as monazite and apatite and, minerals that contain both high REE and heavy (HFSE) elements i.e., heavy minerals. Felsic granites are usually enriched with heavy metal enriched minerals (i.e., heavy minerals) and high REE (McLennan et al., 1993). The Western Ghats in south Kerala are associated with felsic granites and occur at the very proximity to the coast. Therefore, it is likely that the heavy monsoonal rains persuaded both physical and chemical weathering and quick erosion and transport of material by the rivers draining the Western Ghats and then deposition in the lower reaches of rivers and adjacent coastal region. This results in high heavy metal and high REE- enriched minerals in the silt fraction of sediments. Sai Babu et al. (2024) reported PASS-normalized LREE and MREE-enriched and HREE-depleted patterns in both clay and silt fractions of sediments from Kerala and suggested their derivation from felsic granites and laterites from hinterland. In other words, the peak high ∑TE of the silts from south Kerala is related to the source rock geology and relief of the Western Ghats (WG) and, intense chemical and physical weathering of the rocks. Heavy minerals (such as monazite, ilmenite, zircon) enriched sediments have been reported in the coastal region of south Kerala (Mallik et al., 1987).

The broad peaks of high ∑TE in the silts of Maharashtra coincide with peaks of high Co/La, Co/Th ratios (Figure 6D-E) and to some extent peak high Cr/Th ratios (Figure 6f), very low Th/Sc ratio (av. 0.2 compared to 0.9 of UCC; Figure 6G) and high transition trace elements (TTE; (Figure 5; Table 3) and Ti contents relative to PAAS (Figure 3; Table 1). In other words, high ∑TE in the silts of Maharashtra is enriched with TTE-dominant mafic minerals rather than felsic (La and Th) component associated minerals. Major elements data indicated Fe- and Ti-enriched minerals, such as magnetite, ilmenite and rutile. Moreover, the Western Ghats in this region exhibit steep gradient, known as the Great Escarpment of India, and consist of Deccan Trap volcanic rocks. Chemical weathering produces fine-grained detritus, whereas physical weathering and erosion produce coarser material. The peak of high ∑TE in the silt fraction of sediments is most probably related to physical or mechanical erosion and weathering of Deccan Trap material. The Deccan Traps are characteristically enriched with high concentrations of transition trace elements (TTE) and, Ti and Fe-rich minerals. The MREE- and HREE-enriched patterns are characteristic of both clay and silt fractions of sediments from Maharashtra, indicating their derivation from Deccan Trap basalts (Saibabu et al., 2024). Therefore, source rock composition, topography of the WG and associated physical and chemical weathering favoured peak high ∑TE in these sediments. Unlike Kerala, the peak high ∑TE of silts corresponds to low ∑REE in the sediments of Maharashtra (Figure 6A-B) implying basalts are enriched with TTE but not enriched with REE. In other words, peaks of high ∑TE in two different geographic domains associated with silt fractions of sediments are related to the combined influence of source rocks, climate and topography.

5.5. Factors Controlling Th/U and Rb/Sr Ratios—Lithology and Chemical Weathering

Th/U ratio: Trace elements (Th, U, Rb and Sr) content and ratios of Th/U and Rb/Sr can be used to measure the intensity of weathering in the source region. (McLennan et al., 1990; Armstrong et al., 2013; Sahoo et al., 2017; Viers et al., 2000; Nagarajan et al., 2007). Th is immobile in the sedimentary environment, whereas U is strongly mobile and the weathering and recycling are expected to result in oxidation of U to the soluble U^{6+} state (McLennan et al., 1993). The higher Th (mean: 12.8 µg/g) and U (mean: 3.5 µg/g) contents in the clay fraction of sediments from A-P Terrain than in UCC (Th: 10.1 µg/g; U: 2.63 µg/g; Table 2) indicate high Th and U contents from granitic source. The higher mean Th/U ratio (4.1) of the A-P terrain than in UCC (3.8) probably suggests oxidation of U to the soluble U^{6+} (McLennan et al., 1993) and thus the intensity of chemical weathering affected this ratio. Significant positive correlation between Th content and Th/U ratio in both fractions of sediments from A-P terrain (Figure 7B) suggests chemical weathering modified the Th/U ratio. Usually, the Th/U ratio increases with increasing degree of chemical weathering. However, in the sediments of Kerala, the peak high Th/U ratio (Figure 6c) coincides with peak high ΣTE (Figure 6a), suggesting lithology of the source rocks also affected this ratio. Felsic granite are major rock types in south and central Kerala and contain high Th-enriched minerals (Soman 2002). The adsorption of Th by clay minerals produced under strong degree of weathering results in high Th/U ratios (McLennan et al., 1993). Therefore, chemical weathering, lithology of source rocks and adsorption of Th onto clays affected the Th/U ratio in the sediments of Kerala. The mean Th and U contents increase and Th/U ratios decrease as one moves from Kerala to Karnataka and then to Goa in both fractions of sediments (Table 2 and Table 3). In other words, the sediments from Karnataka and Goa gained U and, as a result the Th/U ratios are lower than in UCC (Figure 7A) and do not fall on the weathering trend line shown in Figure 7B. Since the sediments from Karnataka and Goa contain particulates from Fe-Mn ores together with lateritic material, the Th and U contents are influenced by ore material, favouring gaining U, leading to decrease in Th/U ratio of the sediments.

The lower mean Th (8.6 µg/g), U (2.19 µg/g) contents and higher mean Th/U ratio (4.47) for the clay fractions of sediments from DT terrain than in UCC (Tables 2 and 3) imply low Th and U contents in source rocks and strong oxidation of U due to weathering. Weak correlation between Th/U ratio and Th content (Figure 7B) in the clay fractions and moderate correlation in silt fractions of sediments negate that the intensity of weathering is a sole factor influencing Th/U ratio. Moreover, Figure 7B shows nearly all sediments from Gujarat and a few sediments from Maharashtra fall on the weathering trend line. A few sediment samples from Maharashtra gained U resulting in low Th/U ratios and plot below UCC (Figs. 7A and 7B), suggesting contaminated crust material could have affected this ratio. The strong correlation of U with Al_2O_3 and Fe_2O_3 (Table 4) indicate U associated with silicate, Fe-oxy-(hydr)oxides and, weathering of contaminated crustal material with basalts at the transition zone of Goa and Maharashtra may have provided U to the sediments, causing low Th/U ratio. A few sediments from Maharashtra fall within or close to the depleted mantle (Figure 7B), implying these sediments are weathered directly from basalts. In other words, the Th/U ratios of sediments from Maharashtra are affected by chemical weathering of basalts and contaminated crustal source material from hinterland. The Th/U ratios for the clay and silt fractions of sediments from Gujarat are higher than in UCC, and the values plot on the weathering trend line (Figure 7C) suggesting oxidation of U may have enhanced Th/U ratio. However, the sediments from Gujarat exhibit weak to intermediate weathering (Fig, 4A-B) and are compositionally immature (Figure 4C), implying high ratios may not be due to chemical weathering and, recycled sediments may have enhanced the Th/U ratio.

Rb/Sr ratio: Rubidium (Rb) tends to co-exists with K in silicate minerals such as K-feldspar, biotite and muscovite, whereas Sr prefers Ca-bearing minerals such as carbonates, plagioclase and pyroxenes (Liu et al., 2012). Moreover, K-bearing minerals are more stable than Ca-bearing minerals resulting in fractionation between Rb and Sr during weathering (Jin et al. 2005; Liu et al. 2007). The

Preprints.org (www.preprints.org) | NOT PEER-REVIEWED | Posted: 11 October 2024 doi:10.20944/preprints202410.0793.v1

much lower mean Rb and Sr contents of the sediments (Table 2 and 3) than in UCC and PAAS from both terrains imply that some Sr and Rb are lost to solution during chemical weathering. Rubidium (Rb) is highly soluble and also adsorbs abundantly on to clay minerals (Blum and Erel, 1997). High Rb/Sr ratios in the clay fractions than silt fractions of all sediments (Figure 7C) suggest high degree of chemical weathering and very strong sorption capacity of Rb by clay minerals affected this ratio. Elevated concentrations of Rb have been reported in shale and mudstones (Wampler et al., 2012). Increasing Rb/Sr ratios indicate stronger chemical weathering (Yang et al., 2004). Significant negative correlation between Rb/Sr ratio and Sr content of the sediments from both terrains (Figure 7D) suggest that the Rb/Sr ratios are strongly affected by chemical weathering. However, very high Rb/Sr ratios in both fractions of sediments from south Kerala (Figure 7C) could be due to Rb-enriched rocks in the hinterland and chemical weathering. Soman (2002) reported khondalite–granulite–granite rocks intruded by large pegmatites in south and central Kerala and Archean schists and charnockites with mafic granulites in north Kerala. It is known that felsic granites and pegmatites contain Rb-enriched minerals (Soman 2002). Therefore, very high Rb/Sr ratios in south Kerala may have resulted from strong physical and chemical weathering of felsic granites and pegmatites. Relatively low Rb/Sr ratios in the north Kerala may be because of the increasing mafic component with high Sr in the hinterland rocks and more intense weathering.

Peninsular granites and gneisses are important source rocks in the hinterland of Karnataka and Goa. The Rb in metamorphic rocks is largely associated with K-bearing phyllosilicates such as biotite and muscovite (Liu et al. 2007). Rb also substitutes for K^+ in mica (muscovite) and to a lesser extent in K-feldspars. On the other hand, Sr is the most easily be removed from the parent rocks during chemical weathering and carried away as a solute. Therefore, the ion exchange and differential adsorption mechanisms tend to concentrate Rb during weathering causing high Rb/Sr ratios in the clays of Karnataka and Goa. Therefore, high Rb/Sr ratios are related to the source rocks and intense chemical weathering.

High Rb/Sr ratios continued in the clay and silt fractions of sediments in a few rivers of southern Maharashtra (Figure 7C) appear anomalous because surficial rocks are basalts. Since basalts contain high Sr, one would expect low Rb/Sr ratios, as seen in northern Maharashtra. As mentioned in geology of the hinterland, the Proterozoic (peninsular granite and gneisses) rocks laterally change over to Deccan Traps at the border of Maharashtra and Goa (Figure 1). Since the Deccan Trap material is contaminated with crustal sediments at the transition zone of Maharashtra and Goa, high Rb/Sr ratios in the sediments of southern Maharashtra could be due to the weathering of subsurface rocks and their mixing with the products of Deccan Traps at the transition zone. Heavy monsoonal rains and steep slope may have favored exposure of subsurface rocks and their erosion. Sai Babu et al. (2024) reported positive Ce anomaly in the sediments of southern Maharashtra and its absence in the sediments of northern Maharashtra and attributed to the mixing of weathered products from Deccan basalts with crustal rocks at the transition zone.

The Deccan Trap basalts (basic rocks), prominent rock type in Maharashtra and Gujarat, contain high Sr. Mafic rocks weather 2 to 10 times faster than felsic rocks. As mentioned earlier, Sr is most easily be dissolved from the parent rocks during chemical weathering. Sr also substitutes for Ca in carbonates and clays. Despite the above, strong negative correlation between Rb/Sr ratio and Sr content (Figure 7D) suggest chemical weathering is the major process for modifying this ratio. Moreover, the silt fractions of sediments exhibit high Sr concentration and low Rb/Sr ratios (Figure 7C) close to that of UCC, implying source rock influence may have controlled the Rb/Sr ratio.

5.6. Dominance of Mafic/Felsic Source Component in the Sediments

Binary plots and major/trace element ratios: Major elements provide information on rock composition of the original provenance and the effects of sedimentary processes, such as weathering and sorting. Hayashi et al. (1997) reported Al_2O_3/TiO_2 ratios for the mafic (3-8), intermediate (8-21) and felsic source (21-70)- dominated sediments. The mean Al_2O_3/TiO_2 ratio of the clay (18.1) and silt fractions (15.76) from the A-P terrain and, clay fraction (11.27) from DT terrain (Table 1) indicate that these samples represent intermediate composition between felsic and mafic rock sources. However, the mean Al_2O_3/TiO_2 ratio of silts from DT terrain (6.19) indicates the dominance of mafic component. Plot of these values in the binary plot (Figure 9A) of Al_2O_3 versus TiO_2 (Bhatia, 1983) shows that most of the clay and silt fractions from A-P terrain fall in the intermediate region between felsic and mafic provenance, with a few samples falling in the felsic provenance. Within the DT terrain, the clays from Maharashtra fall in the intermediate zone between mafic and felsic, while those from Gujarat fall in the mafic provenance (Figure 9A). The silt fractions of sediments from DT terrain fall in the intermediate region between mafic and felsic provenance.

The mean Fe_2O_3 content was higher and, TiO_2 and MgO contents were lower for the sediments from A-P terrain than in DT terrain. A plot of these values in the TiO_2 versus Fe_2O_3+MgO diagram (Bhatia, 1983) indicates that the sediments from both terrains plot more towards basalts, suggesting dominance of mafic component in all samples (Figure 9B).

Hayashi et al. (1997) reported TiO_2/Zr ratios for mafic igneous rocks (>200), intermediate rocks between mafic and felsic (<200- 55) and felsic igneous rocks (<55). The mean TiO_2/Zr ratios for the clay fraction of sediments from A-P terrain (160) and, clay (99) and silt fractions (88) from DT terrain reveal intermediate composition between mafic and felsic sources (Tables 2 and 3). However, the mean ratio for the silt fraction of sediments from A-P terrain (27.5) points out the dominance of felsic component. The plot of data in the TiO_2 versus Zr diagram indicates that the sediments from A-P terrain plot in the intermediate region between felsic and mafic, with clay fractions more towards mafic region and silt samples more towards felsic region (Figure 9C). The sediments from DT terrain plot in the intermediate zone between mafic and felsic (Figure 9C).

Felsic rocks are enriched with Th, whereas the basic igneous rocks are enriched with Sc and, Th/Sc ratio can chemically differentiate the sediments. Taylor and McLennon (1985) and Bhatia and Crook (1986) reported Th/Sc ratios for the post-Archean (~1), granitic (>1) and Archean and basic rock (<1)-derived sediments. The mean Th/Sc ratios for the clay fractions of sediments (Tables 2 and 3) from A-P terrain (0.566) and DT terrain (0.243) are much lower than PAAS (0.919) and UCC (0.721), suggesting predominant Archean and basic rocks-derived material. Accordingly, most of the clay fractions of sediments from both terrains fall in the mafic region with a few samples falling in the intermediate zone between mafic and felsic in the Th versus Sc plot (Figure 9D). However, the mean Th/Sc ratio of the silts from A-P terrain (0.93) is close to that of PAAS (0.919), but these silts extend from mafic to felsic region in the Th vs Sc plot (Figure 9D), with more samples from Kerala and Karnataka falling in the felsic region and samples from Goa falling in the intermediate zone between mafic and felsic region. The lower mean Th/Sc ratio of the silts from DT terrain (0.391) than UCC suggests the dominance of mafic component. However, these samples extend from mafic to felsic region, with more samples from Maharashtra falling in the mafic region and more samples from Gujarat falling in the felsic region.

The ratios of Cr/Th, Co/Th, Sc/Th and La/Sc relative to UCC have been used to estimate the dominance of mafic and felsic component in the sediments (McLennan et al. 1980). The much higher mean Cr/Th, Co/Th and Sc/Th ratios and, much lower La/Sc ratio than in UCC for the clay fractions of sediments from A-P terrain (Table 2) imply dominance of mafic component. However, in the silt fractions, the mean Cr/Th, Co/Th and La/Sc ratios are much higher and Sc/Th is lower than in UCC (Table 3). Low Sc/Th ratios in the silts could be due to Th-enriched heavy minerals recycled into the sediments. In the case of DT terrain, the much higher Cr/Th, Co/Th and Sc/Th ratios and much lower La/Sc ratios in the clay fractions of sediments than in UCC (Table 2) imply dominance of mafic component. The mean Sc/Th ratio for the silts of Gujarat (0.59; Table 3) is much lower than in UCC (1.39) implying Th-enriched heavy minerals in this fraction.

Ratio-ratio plots of trace elements: The ratio-ratio plots of immobile trace elements are frequently used to understand the dominance of source rock component and sedimentary processes. The ratio-ratio plot of trace element data in the Th/Sc vs. Zr/Sc diagram (Figure 9E) indicates that the clay samples from both terrains plot close to UCC and spread more towards andesite. High Zr concentrations in a few silt samples from Kerala and Karnataka (Table 3) indicate the presence of zircon, a heavy mineral. Moreover, these silt samples plot on the linear line in the Th/Sc vs. Zr/Sc (Figure 9E), representing zircon addition through sediment recycling process or hydrodynamic

 doi:10.20944/preprints202410.0793.v1

transportation process. The Th/Yb and La/Th ratios are also helpful to determine the dominant source components. The mean Th/Yb ratio is much higher and mean La/Th ratio is close to that of UCC for both fractions of sediments from the A-P terrain. The mean Th/Yb and La/Th ratios of both fractions of sediments from DT terrain are close to that of UCC. The ratio-ratio plot of La/Th vs. Th/Yb (Figure 9F) shows intermediate source between mafic and felsic for both clay and silt fractions. The data points from Kerala extend more towards felsic source pointing to dominance of felsic component.

Ternary diagrams: Ternary diagrams using trace metals are helpful to distinguish the dominant trend of the source components in the sediments. In the La-Th-Sc diagram (Bhatia and Crook, 1986; Jahn and Condie, 1995) the clay and silt fractions from A-P terrain extend from granite to basalt, with samples from Kerala are more towards granite, while those from Karnataka plot more towards basalts (Figure 10A). The clay and silt samples from Goa plot in the granodiorite region (Figure 10A). The sediments from DT terrain fall within the region between granodiorite and basalts (Figure 10A).

Figure 10B shows the plot of V, Ni and Thx10 data in the ternary diagram. Sediments from A-P terrain fall in the region between felsic and mafic rocks, with clay fractions plotting more towards mafic source. Some silt samples fall within felsic region and others plot linearly between felsic and mafic region. The clay fractions of sediments from DT terrain plot close to mafic rocks while silt samples plot parallel to V-Thx10 axes and more towards apex V.

Figure 10C shows the plot of Zr, Cr and Ga data in the ternary diagram. All sediment samples plot parallel to the Cr-Zr axes. The major difference between clay and silt samples from A-P terrain is, silt fractions extend from acidic and metamorphic rocks (Zr apex) to the basic rocks, while clay fractions extend from sedimentary rocks to basic rocks and more towards Cr. Similarly, the clay and silt fractions of sediments from DT terrain extend from sedimentary to basic rocks region (Figure 10C). A few silts from DT terrain also fall in the region representing acidic and metamorphic rocks.

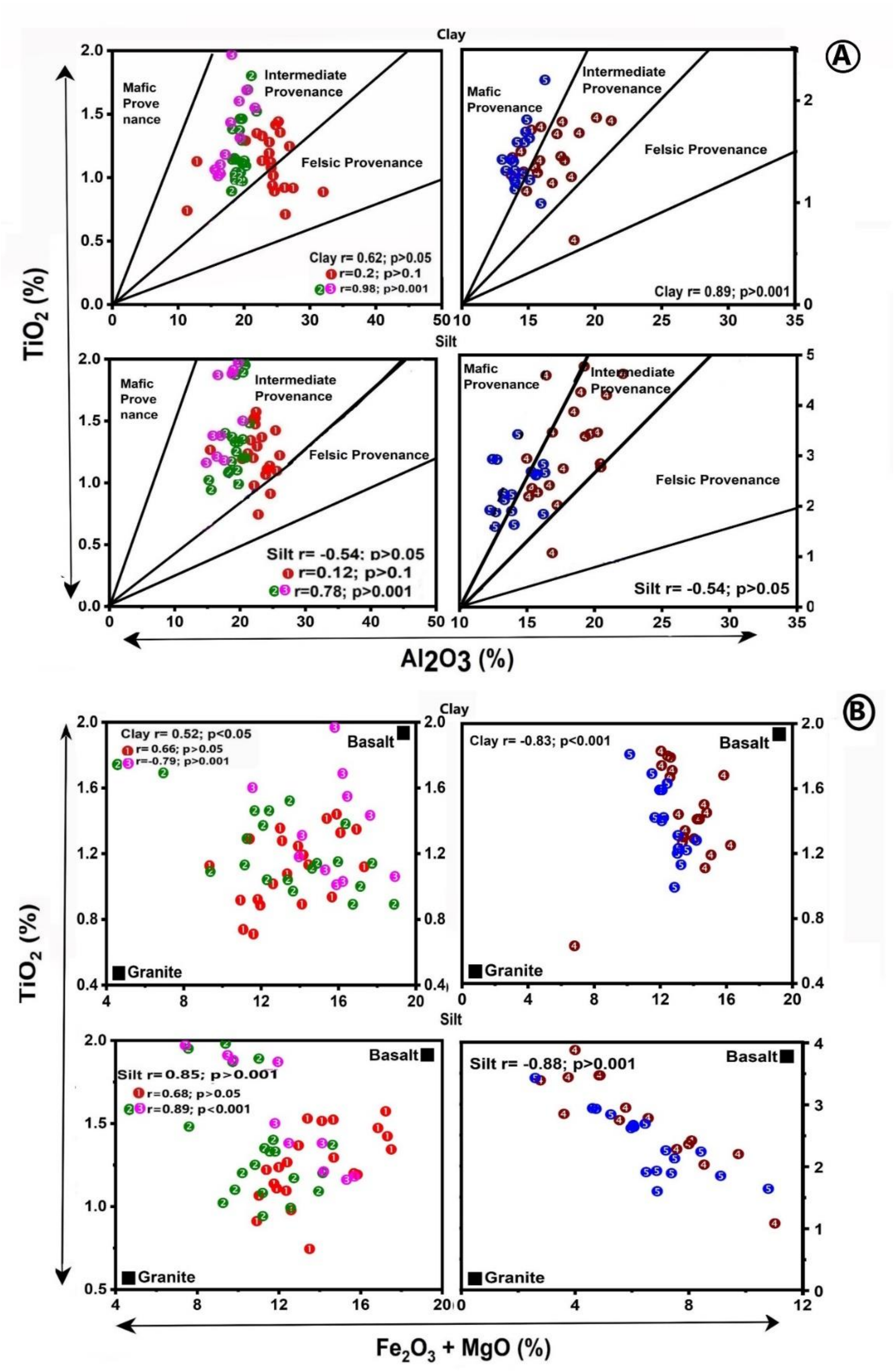
Clay
A
Mafic Prove nance
Intermediate Provenance
Felsic Provenance
Clay r= 0.62; p>0.05
r=0.2; p>0.1
r=0.98; p>0.001
Mafic Provenance
Intermediate Provenance
Felsic Provenance
Clay r= 0.89; p>0.001
Silt
Silt r= -0.54; p>0.05
r=0.12; p>0.1
r=0.78; p>0.001
Silt r= -0.54; p>0.05
TiO2 (%)
Al2O3 (%)
B
Clay r= 0.52; p<0.05
r= 0.66; p>0.05
r=-0.79; p>0.001
Basalt
Granite
Clay r= -0.83; p<0.001
Silt r= 0.85; p>0.001
r=0.68; p>0.05
r=0.89; p<0.001
Silt r= -0.88; p>0.001
Fe2O3 + MgO (%)

Fig. 9

Preprints.org (www.preprints.org) | NOT PEER-REVIEWED | Posted: 11 October 2024 doi:10.20944/preprints202410.0793.v1

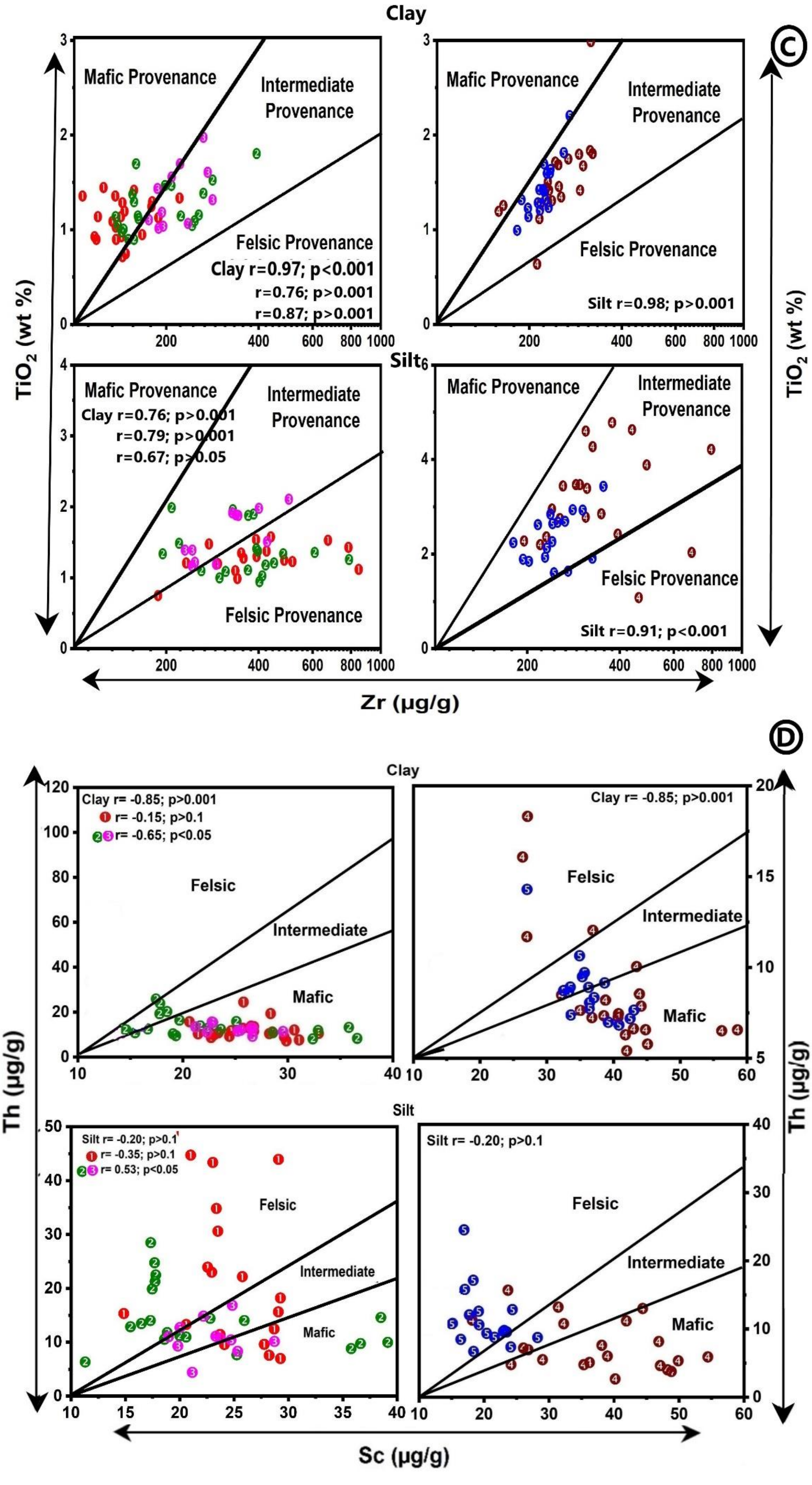

Fig. 9 Cont.

Preprints.org (www.preprints.org) | NOT PEER-REVIEWED | Posted: 11 October 2024 doi:10.20944/preprints202410.0793.v1

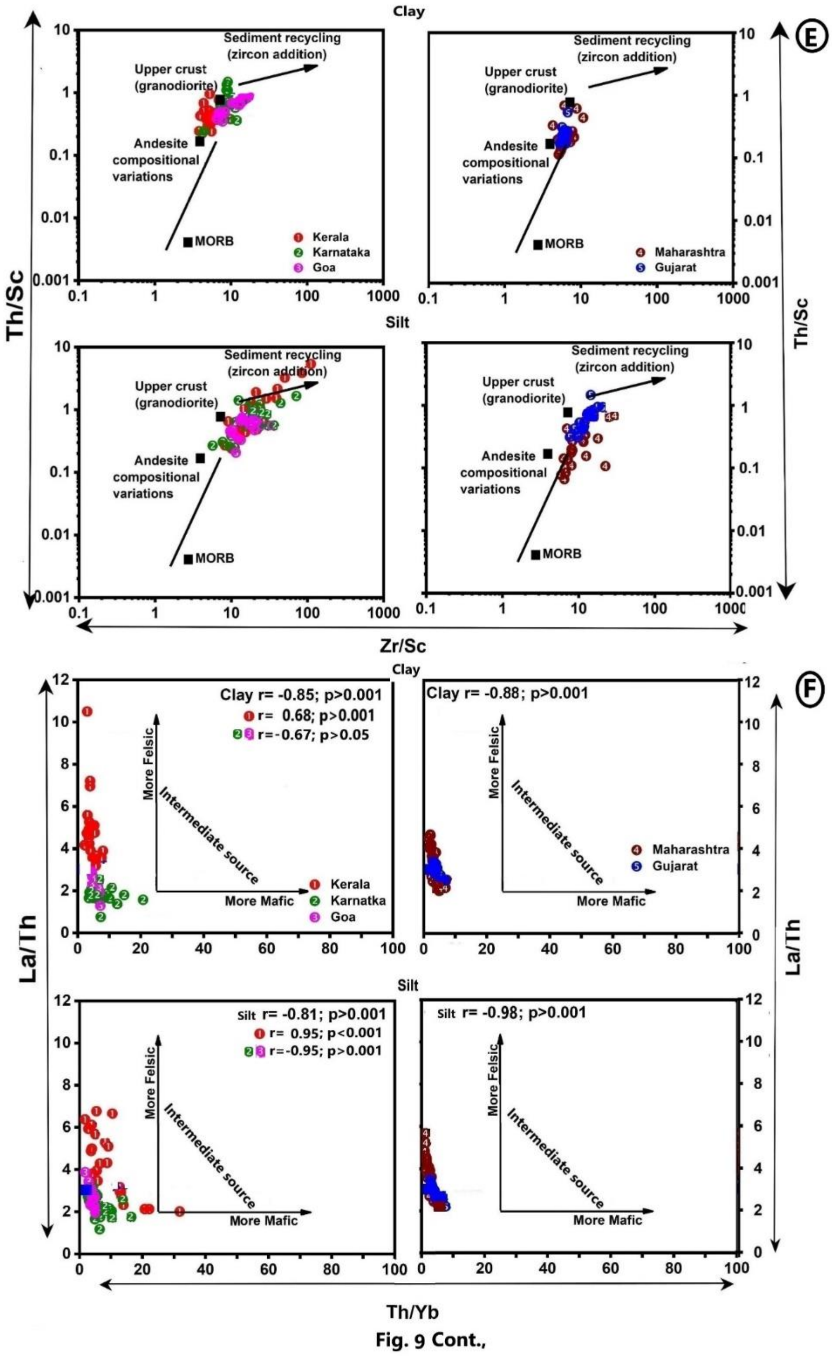

Figure 9. (A) Element-based provenance discrimination diagrams for the clay and silt fraction of river sediments. (A) Al_2O_3 vs. TiO_2; discrimination lines for the felsic, intermediate and mafic provenances are adopted from Bhatia (1983) and Absar and Sreenivas (2015). (B) Fe_2O_3+MgO vs. TiO_2 (after Bhatia, 1983); relationships of (C) Zr vs. TiO2, discrimination lines are after Absar and Sreenivas (2015) and Hayashi et al.(1997) and (D) Th vs Sc (adopted from Cullers, 2002); ratio-ratio plots of (D) Zr/Sc vs. Th/Sc (after from Condie, 1993 and Roser, 2000) and (E) Th/Yb vs. La/Th (adopted from Mongelli et al., 2006).

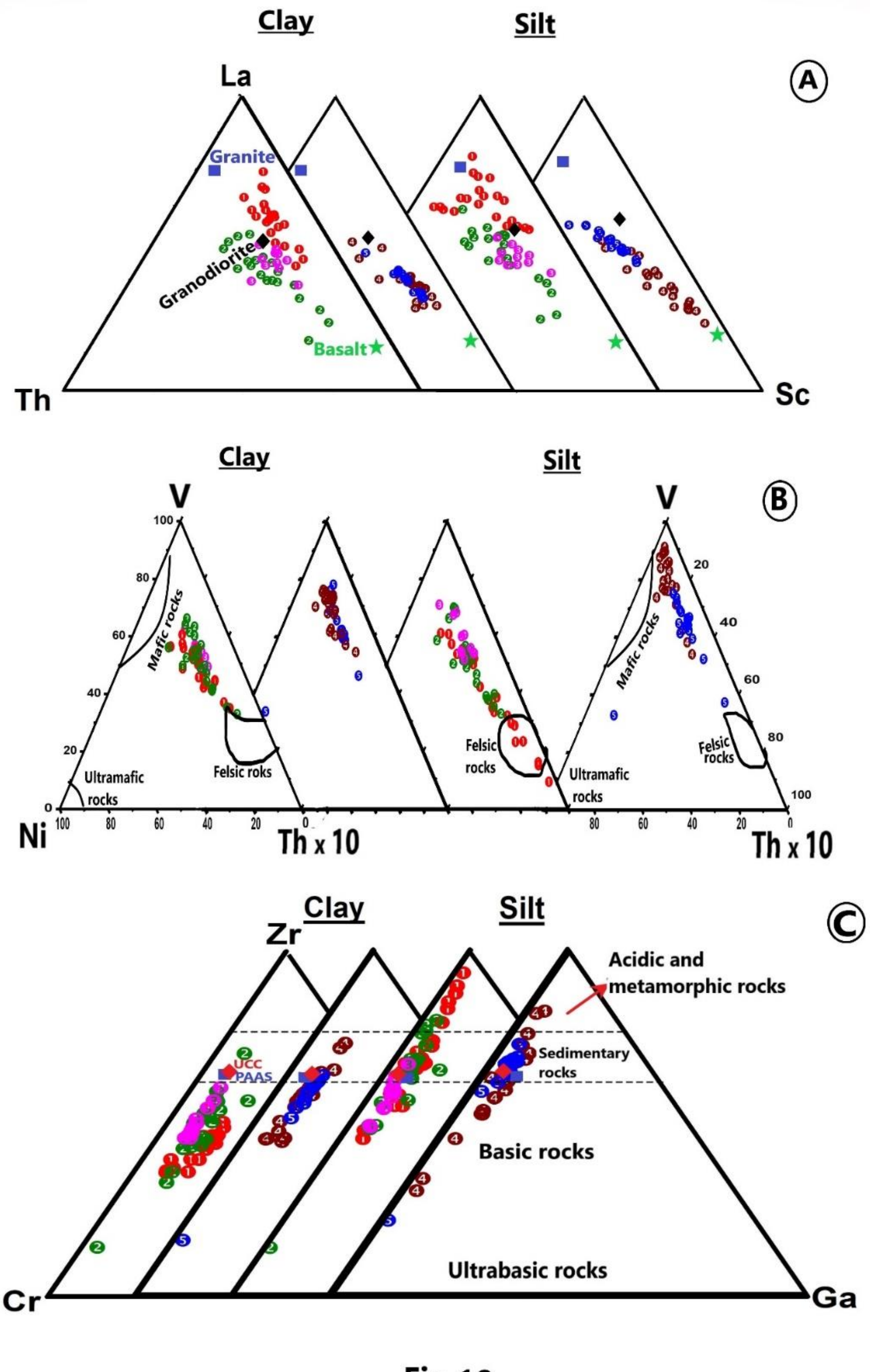

Figure 10. Ternary diagrams using trace elements to demarcate the provenance (A) La–Th–Sc (adopted from Bhatia and Crook, 1986; Bracciali et al., 2007) and (B) V-Ni-Thx10 (adopted from Bracciali et al., 2007) and (C) Zr–Cr–Ga (adopted from Balasubramaniam et al. 1987).

The provenance of river sediments from Figures 9 and 10 may be summarized as follows. The sediments from A-P terrain represent an intermediate provenance between felsic and mafic source. However, the clay fractions from A-P terrain trend more towards mafic composition (Figs. 9B, 9C, 9D, 10B and 10C). A few silt fractions exhibit distinct felsic provenance (9D, 10A, 10B and 10C). Since these silts contain heavy minerals, they may have recycled or transported into the rivers. Similarly, the provenance of sediments from DT terrain is intermediate between felsic and mafic source, with both fractions from Maharashtra and clays from Gujarat trending more towards mafic (9D, 10B and

10C) source. The silts from Gujarat are dominated by felsic source (Figure 9D). Sai Babu et al. (2024) reported mafic component-dominated rare earth elements from the sediments of both terrains. Two implications can be drawn from the provenance of sediments. (a) One would expect the clays from the granitic terrain (A-P terrain) to be more felsic, but mafic component-dominated in the river sediments of Goa, Karnataka and Kerala; it implies crystalline felsic components weathered from granitic terrain may perhaps be deposited more closure to the source and finer mafic component is transported farther from source. The sediments from A-P terrain thus show size sorting during transportation. (b) A curious point one should realize is that the clay fractions from both terrains are more mafic, despite source rocks in the hinterland are different (granitic and basaltic terrains). The sediments from the inner continental shelf all along the west coast of India and Arabian Sea are abundantly clayey (Rao and Wagle, 1997). Since the rivers from the west coast of India are transporting mafic-component dominated clays into the Arabian Sea, it would be a great challenge to identify the exact source of clays weathered from granitic rocks, using trace element chemistry, in the Arabian Sea sediments.

5.7. Summary and Conclusions

Several rivers along the west coast of India drain through the Western Ghats (WG), that comprise of Deccan Trap (DT) terrain in the north and Archean-Proterozoic (A-P) terrain in the south, being weathered under humid, tropical conditions. The basement rocks of the WG are covered by laterites, whose thickness decreases significantly from Kerala (up to 30 m) to Maharashtra (<10 m). The mineralogy and, major and trace elements chemistry of the sediments deposited at the lower reaches of 90 medium and minor rivers from 5 states along the west coast of India were determined to understand the influence of source rocks, intensity of chemical weathering, tectonics and transport processes. Kaolinite is the predominant mineral followed by minor illite and gibbsite and goethite in the sediments from A-P terrain and, smectite followed by kaolinite, chlorite and illite in the sediments from DT terrain. The sediments were depleted with Si, Ca, Mg, Na and K and enriched with Al, Fe, P and Ti relative to that of Post Archean average Australian Shale (PAAS). The sediments from A-P terrain exhibit high Al, Fe and P, while those from DT terrain exhibit high Mg, Ca and Ti. The mean SiO_2/Al_2O_3 ratio (1.45 to 3.29) of sediments from different states suggests that the sediments from A-P terrain resemble lateritic soils, while those from DT terrain are non-lateritic, chemically weathered soils. The weathering indices such as chemical index of alteration (CIA), plagioclase index of alteration (PIA), index of chemical variability (ICV) and mafic index of alteration (MIA) suggest intensely weathered and compositionally mature sediments for Kerala, Karnataka and Maharashtra. The clay and silt fractions of sediments from Goa and clays from Gujarat exhibit intermediate to strong weathering, while the silts from Gujarat are compositionally immature and weakly weathered. Trace elements such as Rb, Sr, Cs and Ba were strongly depleted relative to PAAS in all sediments. The sediments from A-P terrain showed high Th, U, La, Zr and Hf, while those from DT terrain showed high Sc, Cr, Co, Ni, V and Ga compared to PAAS. The mean total trace element content ($\sum$TE) was lower for the clay fraction than their silt fractions of sediments, upper continental crust (UCC) and PAAS. The $\sum$TE of silt fraction exhibits peak high values for Kerala and Maharashtra. The Th/U and Rb/Sr ratios of the sediments are controlled by the lithology of the source rocks and intensity of chemical weathering. The binary plots (Al_2O_3 vs. TiO_2, TiO_2 vs. Fe_2O_3+ MgO, TiO_2 vs. Zr, Th vs. Sc), ratio-ratio plots (Th/Sc vs. Zr/Sc and Th/Yb vs. La/Th) and, ternary diagrams (La-Th-Sc, Zr-Cr-Ga, and V-Ni-Thx10) reveal that the sediments from A-P terrain exhibit intermediate provenance between felsic and mafic source, with clay fractions trending more towards mafic source. Similarly, the sediments from DT terrain represent a provenance intermediate between granodiorite and basalts, with both fractions trending more towards mafic source. The clay fractions exhibiting more of mafic signature from granitic terrain is anomalous and suggest size sorting during transport. Moreover, it would be challenging to identify the source of sediments from the granitic terrain in the Oceans by using trace element chemistry.

Acknowledgments: The authors thank the Vice-chancellor, VFSTR, Vignan's University and Director CSIR-NGRI for their encouragement. This work was carried out under the project 'INSA-Senior Scientist' to VP Rao from the Indian National Science Academy, New Delhi and during Assistant Professor position of Sk. Sai Babu at Vignan's University. We acknowledge these organizations for their financial support.

References

1. Abedini, A.; Calagari, A.A.; and Mikaeili, K. Geochemical characteristics of laterites: The Ailibaltalu Deposit, Iran; Bull. Miner. Res. Explor. ***2014,*** 148 69–84.
2. Absar, N,; Sreenivas, B. Petrology and geochemistry of greywackes of the 1.6 Ga Middle Aravalli Supergroup, northwest India: Evidence for active margin processes. *Int. Geol. Rev.**2015**, 57,* 134–158. https://doi.org/10.1080/00206814. 2014.999355.
3. Amajor, L.C. Major and trace element geochemistry of Albian and Turonian shales from the Southern Benue trough, Nigeria. *J. African Earth Sci.* ***1987****, 6(5),* 633–641.
4. Armstrong-Altrin, J.S,; Nagarajan, R,; Madhavaraju, J,; RosalezHoz, L,; Yong, I.L.L,; Balaram, V,; Cruz-Martınez, A,; AvilaRamırez, G. Geochemistry of the Jurassic and Upper Cretaceous shales from the Molango Region, Hidalgo, eastern Mexico: Implications for source-area weathering, provenance, and tectonic setting. *C. R. Geosci.* ***2013****, 345,* 185–202.
5. Armstrong-Altrin, J.S.; Madhavaraju, J.; Vega-Bautista, F.; Ramos-V'azquez, M.A.; P'erez- Alvarado, B.Y.; Kasper-Zubillaga, J.J.; Bessa, A.Z.E. Mineralogy and geochemistry of Tecolutla and Coatzacoalcos beach sediments, SW Gulf of Mexico. *Appl. Geochem.* ***2021****,134,* 105103.
6. Babechuk, M.G,; Widdowson, M,; Kamber, B.S. Quantifying chemical weathering intensity and trace element release from two contrast ing basalt profiles, Deccan traps, India. *Chem Geo.* ***2014****,363,* 56–75.
7. Babechuk, M.G,; Widdowson, M,; Murphy, M,; Kamber, B.S. A combined Y/Ho, high field strength element (HFSE) and isotope perspective on basalt weathering, Deccan traps, India. *Chem Geol.* **2015**.https://doi.org/10.1016/j.chemgeo.2014.12.017.
8. Babechuk, M,; Fedo, C. Analysis of chemical weathering trends across three compositional dimensions: applications to modern and ancient mafic-rock weathering profiles. *Can J Earth Sci.* **2022**. https://doi.org/10.1139/cjes-2022-0053.
9. Balasubramaniam, K.S, Surendra, M,; Kumar, T.V. Genesis of certain bauxite profiles from India. *Chem. Geol.* ***1987****, 60,* 227–235
10. Bayon, G,; Toucanne, S,; Skonieczny, C,; Andre, L,; Bermell, S,; Cheron, S,; Dennielou, B,; Etoubleau, J,; Freslon, N,; Gauchery, T,; Germain, Y,; Jorry, S.J,; Menot, G,; Monin, L,; Ponzevera, E,; Rouget, M.L,; Tachikawa, K,; Barrat, J.A. Rare earth elements and neodymium isotopes in world river sediments revisited. *Geochim. Cosmochim. Acta.* ***2015****, 170,* 17–38.
11. Berner, R.A.; Berner, E.K. Silicate weathering and climate. In: Ruddiman, W.F. (Ed.), Tectonic Uplift and Climate Change. *Plenum Press, New York.**1997***, 354–365.
12. Bhatia, M.R. Plate tectonics and geochemical composition of sandstones: *Journal of Geology.* ***1983****, 91,* 611–627.
13. Bhatia, M.R.; Crook, K.A.W. Trace element characteristics of graywackes and tectonic setting discrimination of sedimentary basin: *Contributions to Mineralogy and Petrology.* ***1986****, 92,*181–193.
14. Bhuiyan, M.A.H.; Rahman, M.J.J.; Dampare, S.B.; Suzuki, S. Provenance, tectonics and source weathering of modern fluvial sediments of the Brahmaputra-Jamuna River, Bangladesh: Inference from geochemistry. *J. Geochem. Explor.* ***2011****, 111 (3),* 113–137. https://doi.org/10.1016/j.gexplo.2011.06.008.
15. Blum, J.D.; Erel, Y. Rb-Sr isotope systematics of a granitic soil chronosequence: the importance of biotite weathering. *Geochim. Cosmochim. Acta.**1997**, 61,* 3193-3204.
16. Borges, J.B.; Huh, Y.; Moon, S.; Noh, H. Provenance and weathering control on river bed sediments of the eastern Tibetan Plateau and the Russian Far East. *Chem. Geol.* ***2008****, 254* (1–2), 52–72.
17. Boruah, R.; Laskar, J.J. Geochemical characteristics of Neogene sandstones of the East and West Siang Districts of Arunachal Pradesh, NE India: implications for source-area weathering, provenance, and tectonic setting. *Geochim. Cosmochim. Acta.* ***2022****, 41 (1),* 100–120.
18. Bracciali, L,; Marroni, M,; Pandol, B.L,; Rocchi, S,; Arribas, J,; Critelli, S,; Johnsson, M.J. Geochemistry and petrography of Western Tethys Cretaceous sedimentary covers (Corsica and Northern Apennines): From source areas to configuration of margins. *Geol. Soc. Am. Spec. Paper.* ***2007****, 420,* 73–93.
19. Chamley, H. Clay mineralogy. *Springer-Verlag, Germany,* ***1989****,* 623.
20. Chougong, D.T.; Bessa, Z.E.; Ntyam, S.C.; Yongue, R.F.; Ngueutchoua, G.; Armstrong-Altrin, J.S. Mineralogy and geochemistry of Lob´ e River sediments, SW Cameroon: Implications for provenance and weathering. *Journal of African Earth Sciences.* ***2021****,183,*104320.
21. Condie, K.C. Chemical composition and evolution of the upper continental crust: Contrasting results from surface samples and shales: *Chemical Geology*. ***1993****, 104,* 1–37.doi:10.1016/0009-2541(93)90140-E.
22. Cox, R.; Lowe, D.R.; Cullers, R.L. The influence of sediment recycling and basement composition on evolution of mudrock chemistry in the southwestern United States. *Geochim. Cosmochim. Acta.**1995**, 59 (14),* 2919–2940.

23. Cullers, R.L. The controls on the major and trace element variation of shales, siltstones, and sandstones of Pennsylvanian-Permian age from uplifted continental blocks in Colorado to platform sediment in Kansas, USA. *Geochimica et Cosmochimica Acta.* ***1994***, *58(22):* 4955-4972, https://doi.org/10.1016/0016-7037(94)90224-0.
24. Cullers, R. The geochemistry of shales, siltstones and sandstones of Pennsylvanian–Permian age, Colorado, USA: Implications for provenance and metamorphic studies. *Lithos.* ***2000***, *51*, 181–203.
25. Cullers, R.L. Implications of elemental concentrations for provenance, redox conditions, and metamorphic studies of shales and limestones near Pueblo, Co, USA; Chem. *Geol.* ***2002***, *191*, 305–327.
26. Desai, A.G; Arolkar, D.B,; French, D.; Viegas, A,; Vishwanath, T.A. Petrogenesis of the Bondla layered mafic-ultramafic complex Usgaon, Goa. *J Geo Soc India.* ***2009***, *73*, 697–714.
27. Dhoundial, D.P,; Paul, D.K,; Sarkar, A,; Trivedi, J.R,; Gopalan, K,; Potts, P.J. Geochronology and geochemistry of the precambrian granitic r ocks of Goa, SW India. *J Precam Res.**1987***, *36*, 287–302.
28. Du, D.D,; Chen, L.Q,; Bai, Y.H,; Hu, H.P. Variations in rare earth elements with environmental factors in lake surface sediments from 17 lakes in western China. *J Mt Sci.* ***2021***, *18*, *7*. https://doi.org/10.1007/ s11629-020-6040-4.
29. Fedo, C.M.; Wayne Nesbitt, H.; Young, G.M. Unraveling the effects of potassium metasomatism in sedimentary rocks and paleosols, with implications for paleoweathering conditions and provenance. *Geology.* ***1995***, *23 (10)*, 921–924.
30. Fedo, C.M,; Eriksson, K.A,; Krogstad, E.J. Geochemistry of shales from the Archaean (*3.0 Ga) Buhwa greenstone belt, Zimbabwe: Implications for provenance and sourcearea weathering. *Geochim. Cosmochim. Acta.* ***1996***, *60*, 1751–1763, https://doi.org/10.1016/0016-7037(96)00058-0.
31. Folk, R.L. Petrology of the sedimentary rocks. *Hemphills, Austin, TX,* ***1968***, 170.
32. Garzanti, E.; Resentini, A. Provenance control on chemical indices of weathering (Taiwan river sands). *Sed. Geol.* ***2016***, *336*, 81–95.
33. Gokul, A.R,; Srinivasan, M.D,; Gopalakrishnan, K,; Viswanathan, L.S. Stratig raphy and structure of Goa. Seminar volume on Earth resources for Goa's development. *Geo Surv of India,**1985***, 1–13.
34. Gu, X.X,; Liu, J.M,; Zheng, M.H,; Tang, J.X,; Qt. L. Provenance and tectonic setting of the Proterozoic turbidites in Hunan, South China: Geochemical Evidence. *J. Sedim. Res.* ***2002***, *72*, 393–407.
35. Guo, L.; Zhang, H.; Peng, X. Geochemistry and sedimentology of sediments in a short fluvial system, NW China: implications to the provenance and tectonic setting. *Journal of Oceanology and Limnology.* ***2023***, *41*, *5*, 1706-1728. https://doi.org/10.1007/s00343-022-1428-3
36. Gurumurthy, G.P. Geochemical split among the suspended and mud sediments in the Nethravati River: insights to compositional similarity of peninsular gneiss and the Deccan Basalt Derived sediments, and its implications on tracing the provenance in the Indian Ocean. *Geochem Geophys Geosyst*, ***2024***, 25:e2024GC011642. https://doi.org/10.1029/2024GC011642.
37. Hayashi, K.I.; Fujisawa, H.; Holland, H.D.; Ohmoto, H. Geochemistry of~ 1.9 Ga sedimentary rocks from northeastern Labrador, Canada. *Geochim. Cosmochim. Acta.* ***1997***, *61 (19)*, 4115–4137.
38. He, J.; Garzanti, E.; Dinis, P.; Yang, S.; Wang, H. Provenance versus weathering control on sediment composition in tropical monsoonal climate (South China) - 1. Geochemistry and clay mineralogy. *Chem. Geol.* ***2020***, *558*, 119860.
39. Hossain, H.M.; Hasna Hossain, Q.; Kamei, A.; Araoka, D. Compositional variations, chemical weathering, and provenance of sands from the Cox's Bazar and Kuakata beach areas, Bangladesh. *Arabian J. Geosci.* ***2018***, *11 (23)*, 1–17.
40. Hossain, H.M. Major, trace, and REE geochemistry of the Meghna River sediments, Bangladesh: Constraints on weathering and provenance. *Geological Journal.* ***2020***, *55*. https://doi.org/10.1002/gj.3595.
41. Jean, A,; Beauvais, A,; Chordon, D,; Arnaud, N,; Jayananda, M,; Mathe, P.E. Weathering history and landscape evolution of western ghats (India) from 40Ar/39Ar dating of supergene K–Mn oxides. *J. Geol Soc.* ***2020***, *177*, 523–536. https://doi.org/10.1144/jgs2019-048.
42. Jin, W.; Cao, J.; Wu, J.; Wang, S. A Rb/Sr record of catchment weathering response to Holocene climate change in Inner Mongolia. *Earth Surface Processes and Landforms*, ***2005***, DOI: 10.1002/esp.1243.
43. Kale, V. The Western Ghat: The Great Escarpment of India. ***2009.*** 10.1007/978-90-481-3055-9_26.
44. Kaotekwar, A.B,; Rajkumar, R,; Satyanarayana, M,; Keshav Krishna, A,; Charan, S.N. Structures, Petrography and Geochemistr y of Deccan Basalts at Anantagiri Hills, Andhra Pradesh. *J Geol Soc India.* ***2014***, *84*, 675–685.
45. Kessarkar, P.M.; Rao, V.P.; Ahmad, S.M.; Babu, G.A. Clay minerals and Sr–Nd isotopes of sediments along the western margin of India and their implication for sediment provenance. *Mar. Geol.* ***2003***,*202*, 55–69.
46. Kessarkar, P.M,; Suja, S,; Sudheesh, V. Iron ore pollution in Mandovi and Zuari estuarine sediments and its fate after mining ban. *Envi ron Monit Assess.* ***2015***, *187*, 572. https://doi.org/10.1007/s10661-015-4784-z.
47. Krishnan, M.S. Geology of India and Burma. *Madras, Higgin Bothoms,**1968***, 536.
48. Kump, L.R.; Brantley, S.L.; Arthur, M.A. Chemical weathering, atmospheric CO2 and climate. *Annu. Rev. Earth Planet. Sci.* ***2000***, *28*, 611–667.

49. Lightfoot, P.C,; Hawkesworth, C.J,; Devey, C.W,; Rogers, N.W,; van Calsteren, P.W.C. Source and di¡erentia tion of Deccan Trap lavas: imp lications of geochemical and mineral chemical variations. *J Petrol.* ***1990***, 31:1165–1200.
50. Liu, L.; Yu, K.; Li, A.; Zhang, C.; Wang, L.; Liu, X.; Lan, J. Weathering Intensity Response to Climate Change on Decadal Scales: A Record of Rb/Sr Ratios from Chaonaqiu Lake Sediments, Western Chinese Loess Plateau. *Water*, ***2007***, *15,10*, 10.3390/w15101890.
51. Liu, S.; Zhang, J.; Li, Q.; Zhang, L.; Wang, W.; Yang, P. Geochemistry and U-Pb zircon ages of metamorphic volcanic rocks of the Paleoproterozoic Lüliang Complex and constraints on the evolution of the Trans-North China Orogen, North China Craton. *Precambr. Res.* ***2012***, *222*, 173–190.
52. Lupker, M.; France-Lanord, C.; Galy, V.; Lav´ e, J.; Kudrass, H. Increasing chemical weathering in the Himalayan system since the Last Glacial Maximum. *Earth Planet. Sci. Lett.* ***2013***, *365*, 243–252.
53. Maharana, C.; Srivastava, D.; Tripathi, J.K. Geochemistry of sediments of the Peninsular rivers of the Ganga basin and its implication to weathering, sedimentary processes and provenance. *Chem. Geol.* ***2018***, *483*, 1–20.
54. Mallik, T.K,; Vasudevan, V,; Verghese, P.A,; Machado, T. The black sand placer deposits of Kerala, Southwest India. *Mar Geol.* ***1987***, *77*, 129–150.
55. Martin, F.J,; Doyne, H.C. Laterite and lateritic soils in Sierra Leone. *J Agr Sci.* ***1927***, *17*, 530–547.
56. Mascarenhas, A,; Kalavampara, G. Natural resources of Goa: a geological perspective. *Geological Society of Goa, Miramar*, ***2009***, 213. (ISBN: 978-81-908737-0-3).
57. McLennan, S.M.; Taylor, S.R. Th and U in sedimentary rocks: Crustal evolution and sedimentary recycling. *Nature.* ***1980***, *285*, 621–624.
58. McLennan, S.M. Rare earth elements in sedimentary rocks: Influence of provenance and sedimentary processes: *Reviews in Mineralogy.* ***1989***, *21*,169–200.
59. McLennan, S.M,; Taylor, S.R,; McCulloch, M.T,; Maynard, J.B. Geochemistry and Nd–Sr isotopic composition of deepsea turbidites: crustal evolution and plate tectonic associations. *Geochim. Cosmochim. Acta.* ***1990***, *54*, 2014–2050.
60. McLennan, S.M,; Hemming, S,; McDaniel, D.K,; Hanson, G.N. Geochemical approaches to sedimentation, prove nance and tectonics. In: Johnsson JM, Basu A (eds) Processes controlling the composition of clastic sediments. *Geol Soc Am, USA*, ***1993***, *284*,1–21.
61. Naidu, A.S.; Mowatt, T.C.; Somayajulu, B.L.K.; Sreeramachandra Rao, K. Characteristics of clay minerals in the bed loads of major rivers of India. In: Degens, E.T., Kempe, S., Herrera, R. (Eds.), Transport of Carbon and Minerals in Major World Rivers, Pt.3. Mitt. *Geol.-Paläont Inst. Univ., Scope/Unep Sonderbd, Hamburg.* ***1985***, *58*, 559–568.
62. Naqvi, S.M. Geology and evolution of the Indian plate (from Hadean to Holocene 4 Ga to 4 Ka). *Capital Publishing Company, New Delhi*, ***2005***, 450.
63. Narayanaswamy, S. Geochemistry and genesis of laterite in parts of Cannanore District, North Kerala. *PhD thesis, Cochin University of Science and Technology*, ***1992***, 116.
64. Nesbitt, H.w.; Young, G.M. Early Proterozoic climates and plate motions inferred from major element chemistry of lutites. *Nature,* ***1982***, *299 (5885)*, 715–717.
65. Nesbitt, H.W,; Young, G.M. Petrogenesis of sediments in the absence of chemical weathering: effects of abrasion and sorting on bulk composition and mineralogy. *Sediment.* ***1996***, *43*, 341–358.
66. Nesbitt, H.W,; Markovics, G. Weathering of granodiorite crust, long-term storage of elements in weathering profiles, and petrogenesis of siliciclastic sediments. *Geochim Cosmochim Acta.* ***1997***, *61*,1653–1670.
67. Pourmand, A,; Dauphas, N,; Ireland, T.J. A novel extraction chromatography and MC–ICP–MS technique for rapid analysis of REE, sc and Y: revising CI-chondrite and post-archean Australian Shale (PAAS) abundances. *Chem Geol.* ***2012***, *291*,38–54.
68. Prajith, A,; Rao, V.P,; Kessarkar, P.M. Controls on the distri bution and fractionation of yttrium and rare earth elements in core sedimen ts from the Mandovi estuary, western India. *Cont Shelf Res.* ***2015***, *92*, 59–71.
69. Price, J.R,; Velbel, M.A. Chemical weathering indices applied to weathering profiles developed on heterogeneous felsic metamorphic parent rocks. *Chemical Geology*, ***2003***, *202(3-4)*, 397-416, https://doi.org/10.1016/j.chemgeo. 2002.11.001.
70. Pourret, O,; Davranche, M. Rare earth element sorption onto hydrous manganese oxide: a modeling study. *J Colloid Interface Sci.* ***2013***, *395*,18–23.
71. Radhakrishna, B.P. Archaean granite-greenstone terrain of south Indian shield. In: Naqvi SM, Rogers JJW (eds) Precambrian of South India, Geol Soc India Memoir,**1983**, 4, 1–46.
72. Rahman, Md.A.; Das, S.C.; Pownceby,M.I.; Alam, Md.S.; Zaman, M.N. Geochemistry of Recent Brahmaputra River Sediments: Provenance, Tectonics, Source Area Weathering and Depositional Environment. Minerals **2020**, 10, 813; doi:10.3390/min10090813
73. Ramesh, R.; Subramanian, V.; Van Grieken, R.; Van't Dack, L. The elemental chemistry of sediments in the Krishna River basin, India. *Chem. Geol.* ***1989***, *74*, 331–341.
74. Rao, K.L. India's water wealth. *Orient Longman Ltd., New Delhi*, ***1975***, 255.

75. Rao, V.P. and Rao, B. R, Provenance and distribution of clay minerals in the continental shelf and slope sediments of the west coast of India; Cont. Shelf Res. ***1995***, 15 1757–1771.Rao, V.P. and
76. Rao, V. P. and Wagle, B.G. Geomorphology and surBcial geology of the western continental shelf and slope of India: A review; Curr. Sci. **1997**, 73 330–350
77. Roser, B.P. Whole-rock geochemical studies of clastic sedimentary suites. *Memoirs of the Geological Society of Japan*, ***2000***, 57.
78. Roser, B.P.; Korsch, R.J. Determination of tectonic setting of sandstone-mudstone suites using SiO_2 content and K_2O/Na_2O ratio. *J. Geol.**1986**, 94 (5)*, 635–650.
79. Roser, B.P.; Korsch, R.J. Provenance signatures of sandstone-mudstone suites determined using discriminant function analysis of major-element data. *Chem. Geol.* ***1988***, *67 (1–2)*, 119–139.
80. Roy, D.K.; Roser, B.P. Geochemical evolution of the Tertiary succession of the NW shelf, Bengal basin, Bangladesh: Implications for provenance, paleoweathering and Himalayan erosion. *J. Asian Earth Sci.* ***2013***, *78*, 248–262.
81. Rudnick, R.L.; Gao, S.; Holland, H.D.; Turekian, K.K. Composition of the continental crust. *The Crust.* ***2003***, *3*, 1–64.
82. Saha, A.; Roy, D.K.; Idris, A.M.; Khan, R.; Biswas, P.K.; Ornee. T.I.; Tami. Provenance, weathering, climate and tectonic setting of Padma River sediments, Bangladesh: A geo chemical approach. *Catena.* ***2023***, *233*, 107485.
83. Sahoo, P.K,; Guimar, J.T.F,; Souza-Filho, P.W.M,; Sousa da Silva, M,; Nascimento, W.; Jr, Powell, M.A,; Reis, L.S,; Pessenda, L.C.R,; Rodrigues, T.M,; Fonseca da, Silva, D,; Eliodoro Costa, V.Geochemical characterization of the largest upland lake of the Brazilian Amazonia: Impact of provenance and processes. *J. South Am. Earth Sci.* ***2017***, *80*, 541–558.
84. Sai Babu Sk.; Ramana, R.V.; Rao, V.P.; Rammohan, M.; Krishna, A.K.; Sawant, S.; Satyasree, N.; Krishna, A.K. Composition of the peninsular India rivers average clay (PIRAC): a reference sediment composition for the upper crust from peninsular India. *J. Earth Syst. Sci.* ***2020***, *129*, 39.
85. Sai Babu, Sk.; Prajith, A.; Rao, V.P.; Rammohan, M.; Ramana, R.V.; Satyasree, N.S. Composition of river sediments from Kerala, southwest India: Inferences on lateritic weathering. *J Earth Syst Sci.* ***2023***, *132*, 150.
86. Saibabu, Sk.; Rao, V.P.; Satyasree, N.; Ramana, R. V.; Rammohan, M.; and Sawant, S. Mineralogy and geochemistry of the sediments in rivers along the east coast of India: Inferences on weathering and provenance; J. Earth Syst. Sci. ***2021,*** 130 60, https://doi.org/10.1007/s12040-020-01551-5.
87. Sai Babu, Sk.; Rao, V.P.; Rammohan, M. Controls on the distribution and fractionation of rare earth elements in recent sediments from the rivers along the west coast of India. Environmental Earth Sci., ***2024*** 83:547, https://doi.org/10.1007/s12665-024-11842-5
88. Selvaraj, K.; Chen, C.T.A. Moderate chemical weathering of subtropical Taiwan: constraints from solid-phase geochemistry of sediments and sedimentary rocks. *J. Geol.* ***2006***, *114 (1)*, 101–116.
89. Sensarma, S.; Rajamani, V.; Tripathi, J.K. Petrography and geochemical characteristics of the sediments of the small River Hemavati, Southern India: implication for provenance and weathering processes. *Sed. Geol.* ***2008***, *205*, 111–125.
90. Sharma, A.; Rajamani, V. Weathering of charnockite and sediment production in the catchment area of the Cauvery River, southern India. *Sed. Geol.**2001**, 143*, 169–184.
91. Sharma, A,; Sensarma, S,; Kumar, K,; Khanna, P.P,; Saini, N.K. Mineralogy and geochemistry of the Mahi River sediments in tectonically active western India: implications for Deccan large igneous province source, weathering and mobility of elements in a semi-arid climate. *Geochim Cosmochim Acta.* ***2013***, *104*, 63–83. ISSN 0016-7037. https://doi.org/10.1016/j.gca.2012.11.004.
92. Schellmann, W. A new definition of laterites. *Geol. Surv. India Memoir,**1986**, 120*,1–7.
93. Shynu, R,; Rao, V.P,; Kessarkar, P.M,; Rao, T.G. Rare earth elements in suspended and bottom sediments of the Mandovi estuary, central west coast of India: influence of mining. *Estu Coast Shelf Sci.* **2011**, *94*, 355–368.
94. Shynu, R,; Rao, V.P,; Parthiban, G,; Balakrishnan, S,; Narvekar, T,; Kessarkar, P.M. REE in suspended particulate matter and sediment of the Zuari estuary and adjacent shelf, western India: influence of mining and estuarine turbidity. *Mar Geol.* ***2013***, *346*, 326–342.
95. Shynu, R,; Rao, V.P,; Kessarkar, P.M. Major and trace metals in suspended and bottom sediments of the Mandovi and Zuari estuaries: d istribution, source and pollution. *Environ Sci Pollut Res.* ***2017***. https://doi.org/10.1007/s11356-017-0300-z.
96. Singh, P,; Rajamani, V. REE geochemistry of recent clastic sediments from the Kaveri Flood plains, southern India: implication to so urce area weathering and sedimentary processes. *Geochim Cosmochim Acta.* **2001**, *65*, 3093–3108.
97. Viers, J.; Dupré, B.; Raun, J.J.; Deberdt, S.; Angeletti, B.; Ngoupa, J.N.; Michard, A. Major and trace element abundances, and strontium isotopes in the Nyong basin rivers (Cameroon): constraints on chemical weathering processes and elements transport mechanisms in humid tropical environments. *Chem. Geol.* ***2000***,*169 21*, 1-241.

98. Soman, K. Geology of Kerala, 2nd edn. Geological Society of India, Bangalore, **2002**, 335
99. Sreenath, A.V,; Abhilash, S,; Vijaykumar, P. West coast of India's rainfall is becoming more convective. *J. Clim Atmos Sci.* ***2022***, 5. https://doi.org/10.1038/s41612-022-00258-2.
100. Suja, S,; Lina, F,; Rao, V.P. Distribution and fractionation of rare earth elements and Yttrium in suspended and bottom sediments of the Kali estuary, western India. *Environ Earth Sci.* ***2017***, *76*, 174. https://doi.org/10.1007/s12665-017-6497-9.
101. Subramanian, V.; Van't Dack, L.; Van Grieken, R. Chemical composition of river sediments from the Indian subcontinent. *Chem. Geol.**1985***, *48*, 271–279.
102. Taylor, S.R,; McLennan, S.M. The continental crust: Its composition and evolution. *Blackwell Scientific Publications, Palo Alto, CA, USA, Malden,**1985***, 312.
103. Wampler, J.W.; Krogstad, E.J.; Elliott, W.C.; Kahn, B.; Kaplan, D.J. Long-term selective retention of natural Cs and Rb by highly weathered coastal plain soils. *Environm. Sci. Tech.* ***2012***, 46, 3837-3843.
104. Widdowson, M,; Cox, K.G. Uplift and erosion history of the Deccan traps, India: evidence from laterites and drainage patterns of the western ghats and Konkan Coast. *Earth Planet Sci Lett.**1996***, *137*, 57–69.
105. Wronkiewicz, D.J,; Condie, K.C. Geochemistry and provenance of sediments from the Pongola Supergroup, South Africa: evidence for a 3.0-Ga-old continental craton. *Geochimica et Cosmochimica Acta.* ***1989***, *53 (7),* 1537-1549, https://doi.org/10.1016/0016-7037(89)90236-6.
106. Xu, H,; Liu, B,; Wu, F. Spatial and temporal variations of Rb/Sr ratios of the bulk surface sediments in Lake Qinghai. *Geochemical Transactions.* ***2010***, 11-3. doi:10.1186/1467-4866-11-3.
107. Yang, S.Y,; Jung, H.S,; Li, C.X. Two unique weathering regimes in the Changjiang and Huanghe drainage basins: geochemical evidence from river sediments. *Sedimentary Geology,* ***2004a***,*164(1-2),* 19-34, https://doi.org/10.1016/j. sedgeo.2003.08.001.